Westinghouse Electric Company
Nuclear Power Plants
P.O. Box 355
Pittsburgh, Pennsylvania 15230-0355
USA

U.S. Nuclear Regulatory Commission
ATTENTION: Document Control Desk
Washington, D.C. 20555

Direct tel: 412-374-5355
Direct fax: 412-374-5456
e-mail: corletmm@westinghouse.com

Your ref: Docket No. 52-006
Our ref: DCP/NRC1625

September 11, 2003

SUBJECT: Transmittal of Responses to AP1000 DSER Open Items

This letter transmits the Westinghouse responses to Open Items in the AP1000 Design Safety Evaluation Report (DSER) as well as additional open items identified in your letter dated September 3, 2003. A list of the DSER Open Item responses transmitted with this letter is Attachment 1. The non-proprietary responses are provided as Attachment 2 to this letter.

Please contact me at 412-374-5355 if you have any questions concerning this submittal.

Very truly yours,

M. M. Corletti

M. M. Corletti

Passive Plant Projects & Development
AP600 & AP1000 Projects

/Attachments

1. List of the AP1000 Design Certification Review, Draft Safety Evaluation Report Open Item Responses transmitted with letter DCP/NRC1625
2. Non-Proprietary AP1000 Design Certification Review, Draft Safety Evaluation Report Open Item Responses dated September 11, 2003

D063

DCP/NRC1625
Docket No. 52-006

September 11, 2003

Attachment 1

List of

Non-Proprietary Responses

Table 1 "List of Westinghouse's Responses to DSER Open Items Transmitted in DCP/NRC1625"	
3.7.2.3-1 Rev. 1 3.8.5.4-1 Rev. 1 4.5.2-1 6.1-1	

DCP/NRC1625
Docket No. 52-006

September 11, 2003

Attachment 2

AP1000 Design Certification Review
Draft Safety Evaluation Report Open Item Non-Proprietary Responses

AP1000 DESIGN CERTIFICATION REVIEW

Draft Safety Evaluation Report Open Item Response

DSER Open Item Number: 3.7.2.3-1 (Revision 1)

Original RAI Number(s): 230.020, 230.021, 230.022

Summary of Issue:

During the audits conducted on November 12, 2002, and April 2, 2003, the staff discussed with the applicant the development of the dynamic model of the NI structures and reviewed the applicant's analysis reports based on both 3D lumped-mass stick model and 3D finite element model. The seismic analysis results from the 3D finite element model of the coupled auxiliary/shield building shows net tension in the shield building wall. This phenomenon suggests that during the postulated seismic event, parts of the basemat will lift up from the rock surface resulting in changes in the basemat stresses and reduction of shear wall stiffnesses due to reinforced wall cracking. As a result of the detailed review of the seismic modeling approach and analysis methods, the staff identified an issue that the assumptions of uncracked reinforced concrete walls and fixed-base foundation may become invalid. With this finding, the applicant was requested to provide justification to show that the current seismic analysis results used for the design of the NI structures, systems and components are reasonable and acceptable.

In resolving this issue, the staff, during the meeting conducted on April 2, 2003, explained its concern and expectation to the applicant regarding the significance of uplift due to seismic excitation of the NI and the effect of reduction of stiffness of shear walls. The discussion reached the following conclusions:

- The applicant will use East-West lumped-mass stick model of the NI structures supported on a rigid plate with nonlinear springs that transmit reactions in horizontal and vertical directions to simulate the foundation contact area, and perform a seismic time history analysis (the nonlinear springs will be in action only when the rigid plate is in contact with the subgrade). The results of this seismic time history analysis will be compared against the peak accelerations and the floor response spectra at the lumped mass node points obtained from the current three dimensional model analysis without the uplift consideration. If the comparison shows differences, the applicant should evaluate the significance of these differences and their effects on the current seismic design.

- With regard to the effect of shear wall stiffness reduction (due to shear wall cracking) on the seismic analysis results (natural frequencies, peak floor accelerations and the floor response spectra), the applicant will consider using a three dimensional (3D) lumped mass stick model with reduced member stiffnesses to conduct a time history seismic analysis. Results from this analysis will be compared against those currently used by the applicant for the design of the NI structures, systems and components. If the comparison shows differences, the applicant should evaluate the significance of these differences and their effects on the current seismic design.

When the final seismic analyses are performed for the NI structures, the applicant should incorporate the two above discussed effects in the final seismic model for calculating seismic responses. These seismic responses should also be compared against those currently used for the seismic design. If the comparison shows differences on the order of 10 percent or less, the combined effect of uplifting and shear wall cracking will be considered as insignificant. Otherwise, the seismic loads used for the design will have to be revised accordingly.

Depending on the outcome of the comparisons from the two separate analyses discussed above, one for the uplift effect and the other for stiffness reduction, the design calculations for the certified design may have to be revised. This is Open Item 3.7.2.3-1.

Westinghouse Response (Revision 1):

The effects of basemat uplift and shear wall stiffness reduction due to shear wall cracking have been evaluated using seismic time history analyses. Peak accelerations, floor response spectra, and member forces from seismic time history analyses that included basemat uplift and shear wall stiffness reduction effects were compared to seismic time history analyses that did not include these effects. The comparisons described in part A below show that the basemat uplift effect is insignificant. The shear wall stiffness reduction is more significant as describe din part B of below and affects the peak accelerations, the floor response spectra, and time history member forces. The DCD is revised to describe these analyses and the revised results are used for design of the AP1000. The changes in results have been reviewed and do not affect the structural design calculations for the certified design.

A. Liftoff Analysis

Liftoff Model

The effect of liftoff was evaluated using an East-West lumped-mass stick model of the nuclear island structures supported on a rigid basemat with nonlinear springs. This model is shown in Figure 3.7.2.3-1-1 and Figure 3.7.2.3-1-2. The liftoff analysis model consists of the following two elements:

1. The nuclear island (NI) combined stick model (ASB, CIS and SCV).
2. The rigid basemat model with horizontal and vertical rock springs

The size of the equivalent rectangular basemat having the same overturning inertia as the nuclear island basemat is 140.0' × 234.5'. The basemat is modeled as a rigid beam, using 20 elements each 7 feet apart. Hard rock with a shear wave velocity of 8000 feet per second is modeled as horizontal and vertical spring elements with viscous damping at each node of the rigid beam. As shown in Figure 3.7.2.3-1-2, the NI combined stick is attached to the rigid basemat at the NI gravity center, which is about 9 feet from the center of the rigid basemat. In north-south direction, the stick is fixed at the bottom (EL. 60.5'). <u>The stiffness properties of the</u>

ASB and CIS in the NI combined stick model are reduced by a factor of 0.8 to consider the effect of cracking as recommended in Table 6-5 of FEMA 356. This model is a simplified version of the model used in the analyses described in Section B of this response. The three sticks are concentric instead of eccentric and the reactor coolant loop is included as mass only.

Time history analyses are run by direct integration for dead load plus safe shutdown earthquake for two cases:

> "*rocks_dl*" with linear rock springs able to take both tension and compression
>
> "*Liftoff*" with non-linear rock springs where the vertical springs act in compression only and the horizontal springs are active when the vertical spring is closed and inactive when the vertical spring lifts off.

Damping is included as mass and stiffness proportional damping matching the modal damping specified for each structure at frequencies of 3 and 25 Hertz.

Maximum Member Forces and Moments

Table 3.7.2.3-1-1 shows the maximum member forces and moments. Elements 1 to 303 are in the auxiliary and shield building. Elements 401 to 416 are in the containment vessel and elements 500 to 508 are in the containment internal structures. The results show that the liftoff has insignificant effect on the maximum member forces and moments..

Floor Response Spectra

Figure 3.7.2.3-1-3 through Figure 3.7.2.3-1-7 show the floor response spectra in the horizontal and vertical directions at representative elevations of the auxiliary and shield building. The results show that the liftoff effect on the response spectra is insignificant , especially in the horizontal direction. In the vertical direction, especially at the lower elevation, the liftoff effects are visible in the frequency range from 10 to 25 Hz. However the liftoff effect in this range and on the ZPA (zero period acceleration) is insignificant.

Figure 3.7.2.3-1-3 through Figure 3.7.2.3-1-7 also show the case where the soil stiffness has been reduced by 50 percent. This is equivalent to the soil having a shear wave velocity of about 5600 fps. The results show that reducing the soil stiffness leads to lower building response. This is due to the larger displacement of the basemat in the reduced soil stiffness case leading to larger basemat velocities and thus damping in the reduced stiffness soil springs.

Subgrade Pressure and Basemat Displacements

Figure 3.7.2.3-1-8 shows the maximum dynamic subgrade pressure during the analysis. Figure 3.7.2.3-1-9 shows the time history of the pressure at the west and east edge around the time that the peak pressure occurs at the west edge. Lift off has a small effect on the subgrade pressures close to the west edge with insignificant effect beneath most of the equivalent rectangular basemat. The effect on the pressure at the west edge is significantly less than that calculated in the basemat analyses using equivalent static accelerations. Figure 3.7.2.3-1-10 shows basemat displacements at the time of maximum lift off during the time history from dynamic as well as from the equivalent static analyses. The upper figure shows linear analysis results and the lower figure shows non-linear analysis results. In the linear analyses, the differences between dynamic and static displacements are small. The differences are larger in the non-linear analyses. The table below shows the seismic overturning moments and vertical forces in the equivalent static analyses and in the time history analyses at the time that peak pressure occurs at the west edge.

	static (+1.0ew-0.4vt)	*rocks_di* (t=5.685 sec)	Ratio *rocks_di/static*	*liftoff* (t=5.685 sec)	Ratio *liftoff/static*
Vertical Force (kips)	-4.59E+04	-4.69E+04	1.022	-4.64E+04	1.011
Overturning Moment (kips-ft)	1.36E+07	9.04E+06	0.665	9.03E+06	0.664

The overturning moment in the equivalent static analyses is 50% higher than in the dynamic analyses. This conservatism is also seen in Table 3.7.2.3-1-6 and 3.7.2.3-1-8. Thus, the static results from linear analyses using the 100-40-40 method are much more conservative than the dynamic result from non-linear analyses.

Effect of Soil Mass

During the telephone conversation of mid August, 2003, the NRC staff commented that the "slapping" phenomenon that occurs during liftoff was not being addressed fully because the existing liftoff model did not include independently acting soil masses.

In order to investigate the effect of soil mass, gap elements representing soil 80 feet deep were added to the existing liftoff model as shown in Figures 3.7.2.3-1-11. The horizontal and vertical floor response spectra at representative elevations of the auxiliary and shield building are shown in Figures 3.7.2.3-1-12 through 3.7.2.3-1-15. The results show that the soil mass effects are insignificant in the horizontal direction. These effects are also insignificant in the vertical direction at the higher elevations, and are very small at the lower elevations.

Figure 3.7.2.3-1-16 shows comparison of the vertical subgrade pressures at basemat edges for the 0.3g SSE input. These time history plots are shown around the time when the peak toe pressure occurs at the west edge or the peak lift off occurs at the east edge. The plots show slightly higher additional reactions due to slapping at the heel edge (the east edge), but this does not have significant effect on the peak toe pressures at the west edge. The peak toe pressure of the soil-mass model is 28.0 ksf, which is almost the same as the toe pressure of 27.8 ksf obtained by the liftoff model without soil mass.

Figure 3.7.2.3-1-17 shows vertical response time histories of the heel edge (the east edge). The figure shows vertical deflection, relative velocity, and relative acceleration. The slapping effect is noticeable but not significant.

B. Reduced Shear Wall Stiffness

The effects of shear wall stiffness reduction (due to shear wall cracking) were evaluated by changing the concrete modulus in the auxiliary and shield building and the containment internal structure in the nuclear island time history seismic analyses. The stiffness properties are reduced by a factor of 0.8 to consider the effect of cracking as recommended in Table 6-5 of FEMA 356. The revised models also include the changes described in response revision 3 to RAI 230.018.

The results from the seismic time history analyses including the shear wall stiffness reduction effects were compared to results of the seismic time history analyses included in DCD Revision 3 that did not include these effects. The comparison, which is discussed further in subsequent paragraphs, shows that the shear wall stiffness reduction affects the peak accelerations, the floor response spectra, and time history member forces. The reduced stiffness case is considered to provide a better estimate of response than the previous analyses with uncracked concrete. The DCD is therefore being revised to incorporate the results of the new analyses. Comparison tables are provided in this Open Item response together with evaluation of the effect on the structural design previously reviewed by the NRC staff.

Maximum absolute accelerations are compared in Table 3.7.2.3-1- 2 to Table 3.7.2.3-1- 4. The differences are due to the reduction in stiffness as well as to the changes in the model described in the response to RAI 230.018.

Member forces in the revised time history analyses are compared in Table 3.7.2.3-1- 1 to Table 3.7.2.3-1-7 against those from a static analysis of the revised stick model using the equivalent static accelerations used in the auxiliary building equivalent static analyses. The results show that the equivalent static analysis is still conservative for the member forces in the stick model for the Auxiliary and Shield Building and for the Containment Internal Structures. These member forces provide a good measure of the effect on the in-plane forces in the walls and floor slabs. Out of plane forces are dependent on the maximum absolute acceleration. The wall design is generally controlled by in-plane seismic loads. The floors are generally controlled by normal loads. Hence the design using the results of the equivalent static analyses does not need to be revised. Design calculations for critical sections will be reviewed to confirm acceptability for the changes in response when the maximum absolute accelerations in the stick models increased by more than 10% or when the existing calculations consider amplification due to flexibility. The design calculation for nuclear island stability was reviewed and found to be acceptable for the changes in response.

The results show a small increase (up to 10%) in the accelerations for the SCV in the east west direction and larger increases in the north-south and vertical directions (up to 20%). The overturning moments at the base of containment in the equivalent static analyses are 0.87 times those in the revised time history analysis. This increase in seismic response will be addressed in the response to DSER Open Item 3.8.2.1-1

Design Control Document (DCD) Revision:

1. Subsection 3.7.2.2, second paragraph, first two sentences are combined to read:

   The time history seismic analysis of the nuclear island considers 200 vibration modes, extending up to a frequency of 83.8 hertz as shown in Table 3.7.2-4.

2. Add new paragraph at end of subsection 3.7.2.3:

   The finite element models of the coupled shield and auxiliary buildings and the containment internal structures are based on the gross concrete section with the modulus based on the specified compressive strength of concrete. When the finite element or stick models of these buildings are used in time history or response spectrum dynamic analyses, the stiffness properties are reduced by a factor of 0.8 to consider the effect of cracking as recommended in Table 6-5 of FEMA 356 (Reference 5).

3. In Section 3.7.6, reference 5 is added:

   "5. FEMA 356 – Pre-standard and Commentary for the Seismic Rehabilitation of Buildings, November 2000."

4. Revise Table 3.7.2-1 and Tables 3.7.2-4 to 3.7.2-13 to incorporate revised analyses results that include shear wall stiffness reduction.

5. Revise Figure 3.7.2-9, Figure 3.7.2-11, and Figures 3.7.2-15 to 3.7.2-17 to incorporate revised analyses results that include shear wall stiffness reduction.

PRA Revision:

None

Table 3.7.2.3-1-1: Maximum Seismic Member Forces and Moments

Elem	Elevations		rocks_di			liftoff			Ratio Liftoff/rocks_di		
			Axial	Shear	M	Axial	Shear	M			
1	60.50	66.50	47.34	50.65	5020.9	46.58	52.94	4982.3	0.984	1.045	0.992
2	66.50	81.50	16.05	10.54	2634.2	15.76	10.83	2616.0	0.982	1.028	0.993
3	81.50	91.50	53.57	14.24	6474.3	52.10	14.31	6453.8	0.973	1.005	0.997
4	91.50	99.00	49.52	12.20	6340.9	48.23	11.96	6307.9	0.974	0.980	0.995
5	99.00	106.17	46.34	54.86	6253.7	45.22	54.49	6195.8	0.976	0.993	0.991
6	106.17	116.50	44.23	53.50	5884.3	43.25	53.18	5783.9	0.978	0.994	0.983
7	116.50	134.87	39.33	48.07	5366.4	38.71	48.04	5222.2	0.984	0.999	0.973
31	134.87	145.37	34.35	40.81	4592.7	34.15	40.87	4532.8	0.994	1.001	0.987
32	145.37	153.98	32.44	37.66	4210.7	32.39	37.75	4193.3	0.998	1.002	0.996
33	153.98	164.51	30.52	34.71	3929.2	30.34	33.80	3912.9	0.994	0.974	0.996
34	164.51	179.56	28.77	31.99	3591.0	28.64	30.84	3576.2	0.995	0.964	0.996
35	179.56	200.00	26.46	28.88	3110.1	26.44	28.75	3097.4	0.999	0.995	0.996
36	200.00	220.00	24.82	27.39	2482.6	24.80	27.26	2477.4	0.999	0.995	0.998
37	220.00	242.50	22.93	24.87	1918.2	22.85	24.82	1889.7	0.997	0.998	0.985
38	242.50	265.00	20.77	21.41	1337.2	20.68	21.13	1336.5	0.996	0.987	0.999
301	265.00	295.23	17.53	15.77	896.0	17.60	15.88	900.3	1.004	1.007	1.005
303	295.23	333.13	3.08	6.82	277.6	3.09	7.00	284.3	1.003	1.026	1.024
401	100.00	104.12	4.05	6.85	869.5	3.94	6.77	867.2	0.973	0.988	0.997
402	104.12	110.50	4.02	6.80	840.7	3.89	6.72	838.7	0.968	0.988	0.998
403	110.50	112.50	4.02	6.80	797.4	3.89	6.72	795.8	0.968	0.988	0.998
405	112.50	131.68	3.90	6.63	781.6	3.75	6.56	780.1	0.962	0.989	0.998
406	131.68	138.58	3.71	6.39	650.6	3.58	6.32	650.4	0.965	0.989	1.000
407	138.58	141.50	3.71	6.39	606.5	3.58	6.32	606.8	0.965	0.989	1.000
408	141.50	162.00	3.51	6.11	583.4	3.38	6.05	583.7	0.963	0.990	1.001
409	162.00	169.93	3.26	5.73	452.5	3.15	5.69	453.7	0.966	0.993	1.003
410	169.93	200.00	2.84	5.09	397.3	2.75	5.06	398.5	0.968	0.994	1.003
411	200.00	224.00	2.36	4.22	232.6	2.29	4.21	234.3	0.970	0.998	1.007
412	224.00	244.21	1.32	2.59	114.2	1.27	2.60	115.4	0.962	1.004	1.011
413	244.21	255.02	1.00	1.90	54.4	1.00	1.90	55.2	1.000	1.000	1.015
414	255.02	265.83	0.76	1.36	29.0	0.78	1.37	29.4	1.026	1.007	1.014
415	265.83	273.83	0.51	0.84	11.1	0.53	0.85	11.2	1.039	1.012	1.009
416	273.83	281.90	0.21	0.31	2.5	0.22	0.31	2.5	1.048	1.000	1.000
500	60.50	66.50	46.41	35.78	4344.1	45.66	37.40	4310.9	0.984	1.045	0.992
501	66.50	82.50	65.96	66.94	6267.2	64.75	67.80	6220.9	0.982	1.013	0.993
502	82.50	98.00	17.05	55.76	1668.4	17.07	55.30	1674.0	1.001	0.992	1.003
503	98.00	103.00	8.82	16.38	628.0	8.80	16.45	628.9	0.998	1.004	1.001
504	103.00	107.17	5.84	14.44	544.0	5.84	14.52	544.5	1.000	1.006	1.001
505	107.17	134.25	3.24	11.75	478.8	3.33	11.62	479.0	1.028	0.989	1.000
506	134.25	153.00	0.16	1.64	31.2	0.17	1.60	30.5	1.063	0.976	0.978
507	134.25	153.00	0.45	4.78	124.7	0.47	4.76	125.0	1.044	0.996	1.002
508	153.00	169.00	0.11	1.99	32.9	0.11	1.99	32.9	1.000	1.000	1.000

Table 3.7.2.3-1-2: COMPARISON OF SEISMIC RESPONSES AUXILIARY AND SHIELD

MAXIMUM ABSOLUTE NODAL ACCELERATION (ZPA)
COUPLED AUXILIARY & SHIELD BUILDINGS

Elevation (ft)	Maximum Absolute Nodal Acceleration, ZPA (g)					
	N-S Direction		E-W Direction		Vertical Direction	
	100% E	80% E	100% E	80% E	100% E	80% E
333.13	1.36	1.46	1.77	1.51	0.96	1.01
295.23	1.07	1.12	1.24	1.10	0.95	1.00
265.00	0.9	0.91	0.9	0.97	0.58	0.71
242.50	0.81	0.81	0.82	0.89	0.56	0.69
220.00	0.74	0.71	0.75	0.80	0.52	0.65
200.00	0.68	0.71	0.7	0.77	0.48	0.59
179.56	0.6	0.76	0.71	0.78	0.43	0.52
164.51	0.55	0.73	0.69	0.75	0.39	0.48
153.98	0.53	0.70	0.67	0.73	0.39	0.44
134.87	0.5	0.60	0.59	0.63	0.39	0.41
116.50	0.45	0.50	0.47	0.50	0.34	0.37
99.00	0.37	0.39	0.41	0.40	0.33	0.34
81.50	0.32	0.33	0.33	0.33	0.31	0.31
66.50	0.3	0.30	0.3	0.30	0.3	0.30

Table 3.7.2.3-1-3: COMPARISON OF SEISMIC RESPONSES CONTAINMENT VESSEL

MAXIMUM ABSOLUTE NODAL ACCELERATION (ZPA)
STEEL CONTAINMENT VESSEL

Elevation (ft)	Maximum Absolute Nodal Acceleration, ZPA (g)					
	N-S Direction		E-W Direction		Vertical Direction	
	100% E	80% E	100% E	80% E	100% E	80% E
281.90	1.27	1.48	1.42	1.56	1.13	1.25
273.83	1.22	1.43	1.38	1.50	0.85	1.02
265.83	1.17	1.38	1.34	1.43	0.71	0.85
255.02	1.1	1.31	1.28	1.34	0.62	0.73
244.21	1.03	1.23	1.22	1.26	0.58	0.68
224.00	0.9	1.09	1.09	1.11	0.56	0.66
200.00	0.76	0.90	0.93	0.94	0.52	0.61
169.93	0.63	0.69	0.7	0.72	0.46	0.53
162.00	0.59	0.63	0.64	0.67	0.45	0.51
141.50	0.47	0.49	0.53	0.54	0.4	0.45
131.68	0.41	0.43	0.49	0.47	0.38	0.41
112.50	0.37	0.40	0.41	0.37	0.34	0.35
104.12	0.37	0.38	0.39	0.38	0.34	0.32
100.00	0.36	0.38	0.4	0.39	0.33	0.31

Table 3.7.2.3-1-4: COMPARISON OF SEISMIC RESPONSES AUXILIARY AND SHIELD

MAXIMUM ABSOLUTE NODAL ACCELERATION (ZPA)
CONTAINMENT INTERNAL STRUCTURES

Elevation (ft)	Maximum Absolute Nodal Acceleration, ZPA (g) N-S Direction		E-W Direction		Vertical Direction	
	100% E	80% E	100% E	80% E	100% E	80% E
169.00 (PRZ Compartment)	1.33	1.27	1.44	1.64	0.43	0.49
153.00 (SG-West Compartment)	0.73	0.75	0.65	0.71	0.39	0.42
153.00 (SG-East Compartment)	1.15	0.75	0.59	0.78	0.4	0.48
134.25	0.56	0.60	0.51	0.56	0.32	0.35
107.17	0.38	0.40	0.41	0.40	0.31	0.31
103.00	0.37	0.39	0.4	0.40	0.31	0.31
98.00	0.36	0.38	0.39	0.39	0.3	0.31
82.50	0.32	0.33	0.33	0.33	0.3	0.30
66.50	0.3	0.30	0.3	0.30	0.3	0.30

Table 3.7.2.3-1-5

MEMBER FORCES
AUXILIARY AND SHIELD BUILDING

AXIAL AND SHEAR FORCES($x10^3$ Kips)

			Equivalent static			Time history			Ratio Equivalent static / Time history		
Elem	Elev	Elev	Axial	N-S Shear	E-W Shear	Axial	N-S Shear	E-W Shear	Axial	N-S Shear	E-W Shear
303	295.23	333.13	2.81	6.22	7.97	2.81	6.53	6.42	1.001	0.952	1.242
301	265	295.23	16.05	15.51	18.74	16.02	16.27	15.47	1.002	0.953	1.211
38	242.5	265	20.36	22.17	25.45	18.60	22.38	21.16	1.095	0.991	1.203
37	220	242.5	22.89	25.84	29.14	20.59	25.51	24.71	1.112	1.013	1.179
36	200	220	25.10	29.01	32.31	22.41	28.04	27.13	1.120	1.035	1.191
35	179.56	200	27.02	31.78	35.14	23.96	30.08	28.66	1.128	1.056	1.226
34	164.51	179.56	28.56	27.00	27.26	25.13	24.65	21.70	1.136	1.095	1.256
33	153.98	164.51	30.70	18.70	28.44	26.97	16.47	22.76	1.138	1.135	1.249
32	145.37	153.98	33.57	14.43	18.92	28.55	12.15	15.26	1.176	1.188	1.240
31	134.87	145.37	35.59	17.28	22.29	30.40	13.91	18.31	1.171	1.242	1.217
13	134.87	179.56	1.55	8.74	12.54	0.00	8.11	10.10		1.077	1.241
10	134.87	164.51	0.00	11.43	2.44	0.00	10.09	1.94		1.132	1.260
8	134.87	153.86	0.00	7.59	13.95	0.00	6.39	11.65		1.187	1.198
7	116.5	134.88	42.21	51.99	59.21	36.10	42.65	47.85	1.169	1.219	1.237
6	106.17	116.5	47.30	60.55	68.16	40.83	47.41	53.69	1.158	1.277	1.269
5	99	106.17	49.54	63.27	71.05	43.02	48.80	55.11	1.151	1.297	1.289
4	91.5	99	53.00	32.84	23.97	46.51	22.53	14.61	1.140	1.457	1.640
3	81.5	91.5	57.51	36.32	27.75	50.80	25.88	16.83	1.132	1.404	1.649
2	66.5	81.5	44.19	21.74	16.63	35.32	15.68	10.27	1.251	1.386	1.619
1	60.5	66.5	119.58	77.12	82.49	77.90	51.35	47.75	1.535	1.502	1.727

Table 3.7.2.3-1-6

MEMBER FORCES
AUXILIARY AND SHIELD BUILDING

MOMENTS (x10^3 Kips feet)

Elem	Elev	Elev	Equivalent static about N-S Axis	Equivalent static about E-W Axis	Time history about N-S Axis	Time history about E-W Axis	Ratio Equivalent static / Time history about N-S Axis	Ratio Equivalent static / Time history about E-W Axis
303	295.23	333.13	302.10	235.57	266.61	260.99	1.133	0.903
301	265	295.23	868.53	704.41	854.17	872.74	1.017	0.807
38	242.5	265	1441.23	1203.32	1315.66	1374.77	1.095	0.875
37	220	242.5	2096.78	1784.77	1921.62	1989.93	1.091	0.897
36	200	220	2742.99	2365.02	2506.10	2583.91	1.095	0.915
35	179.56	200	3461.27	3014.57	3127.81	3222.60	1.107	0.935
34	164.51	179.56	3870.89	3420.90	3479.65	3608.09	1.112	0.948
33	153.98	164.51	4170.66	3617.62	3723.93	3806.91	1.120	0.950
32	145.37	153.98	4337.07	3745.47	3860.23	4070.55	1.124	0.920
31	134.87	145.37	4573.00	3925.84	3992.65	4257.40	1.145	0.922
13	134.87	179.56	560.22	390.37	451.41	362.38	1.241	1.077
10	134.87	164.51	72.45	338.68	57.41	299.15	1.262	1.132
8	134.87	153.86	264.93	144.06	221.24	121.32	1.197	1.187
7	116.5	134.88	6547.51	5774.79	5428.61	6202.96	1.206	0.931
6	106.17	116.5	7250.37	6392.29	5991.64	6762.95	1.210	0.945
5	99	106.17	7759.36	6843.29	6373.05	7146.70	1.218	0.958
4	91.5	99	7941.96	7079.12	6481.29	7287.50	1.225	0.971
3	81.5	91.5	8217.88	7439.93	6613.75	7499.97	1.243	0.992
2	66.5	81.5	3627.37	4673.08	2474.44	3855.10	1.466	1.212
1	60.5	66.5	4775.48	11391.0	3295.23	9050.29	1.449	1.259

Table 3.7.2.3-1-7

MEMBER FORCES
STEEL CONTAINMENT VESSEL
AXIAL AND SHEAR FORCES($x10^3$ Kips)

			Equivalent static			Time history			Ratio Equivalent static / Time history		
Elem	Elev	Elev	Axial	N-S Shear	E-W Shear	Axial	N-S Shear	E-W Shear	Axial	N-S Shear	E-W Shear
416	273.83	281.9	0.20	0.23	0.26	0.24	0.27	0.28	0.846	0.848	0.918
415	265.83	273.83	0.48	0.62	0.71	0.60	0.73	0.77	0.798	0.853	0.916
414	255.02	265.83	0.71	1.01	1.15	0.88	1.19	1.25	0.811	0.849	0.918
413	244.21	255.02	0.94	1.41	1.61	1.16	1.66	1.73	0.809	0.849	0.931
412	224	244.21	1.23	1.93	2.23	1.53	2.28	2.36	0.805	0.848	0.944
411	200	224	2.78	4.55	4.88	2.80	4.81	4.23	0.991	0.945	1.154
410	169.93	200	3.25	5.24	5.72	3.36	5.60	5.00	0.968	0.935	1.145
409	162	169.93	3.68	5.82	6.38	3.83	6.19	5.57	0.962	0.941	1.145
408	141.5	162	3.95	6.17	6.76	4.11	6.52	5.89	0.960	0.946	1.147
407	138.58	141.5	4.16	6.42	7.03	4.36	6.76	6.11	0.954	0.949	1.151
406	131.68	138.58	4.18	6.44	7.06	4.36	6.76	6.11	0.959	0.953	1.155
405	112.5	131.68	4.40	6.68	7.34	4.61	6.96	6.30	0.954	0.959	1.165
403	110.5	112.5	4.55	6.84	7.52	4.79	7.07	6.37	0.950	0.968	1.181
402	104.12	110.5	4.57	6.86	7.54	4.79	7.07	6.37	0.954	0.970	1.184
401	100	104.12	4.63	6.93	7.61	4.86	7.10	6.40	0.953	0.975	1.189

MOMENTS ($x10^3$ Kips feet)

			Equivalent static		Time history		Ratio Equivalent static / Time history	
Elem	Elev	Elev	about N-S Axis	about E-W Axis	about N-S Axis	about E-W Axis	about N-S Axis	about E-W Axis
416	273.83	281.9	2.075	1.845	2.29	2.16	0.906	0.854
415	265.83	273.83	7.711	6.83	10.26	9.54	0.752	0.716
414	255.02	265.83	20.121	17.755	26.95	25.1	0.747	0.707
413	244.21	255.02	37.545	33.005	50.45	47.1	0.744	0.701
412	224	244.21	82.568	72.08	105.31	99.26	0.784	0.726
411	200	224	214.404	199.186	215.37	249.37	0.996	0.799
410	169.93	200	386.513	356.572	365.53	427.69	1.057	0.834
409	162	169.93	437.078	402.717	416.28	485.37	1.050	0.830
408	141.5	162	575.587	529.175	541.12	624.26	1.064	0.848
407	138.58	141.5	596.103	547.898	561.81	647.61	1.061	0.846
406	131.68	138.58	644.856	592.353	604.02	694.26	1.068	0.853
405	112.5	131.68	785.593	720.385	727.75	831.63	1.079	0.866
403	110.5	112.5	800.639	734.061	741.5	848.17	1.080	0.865
402	104.12	110.5	848.726	777.793	782.14	893.22	1.085	0.871
401	100	104.12	880.124	806.36	808.94	923.25	1.088	0.873

Table 3.7.2.3-1-8

MEMBER FORCES
CONTAINMENT INTERNAL STRUCTURES

AXIAL AND SHEAR FORCES($x10^3$ Kips)

Elem	Elev	Elev	Equivalent static Axial	Equivalent static N-S Shear	Equivalent static E-W Shear	Time history Axial	Time history N-S Shear	Time history E-W Shear	Ratio Equivalent static / Time history Axial	Ratio N-S Shear	Ratio E-W Shear
555	163.79	169	0.01	0.45	0.49	0.01	0.39	0.52	0.900	1.164	0.942
508	153	163.79	0.15	0.63	0.66	0.14	0.55	0.72	1.036	1.145	0.918
507	134.25	153	0.59	1.47	2.92	0.52	1.20	2.13	1.129	1.226	1.369
506	134.25	153	0.21	0.61	2.21	0.15	0.68	2.32	1.400	0.891	0.952
554	121.5	134.25	2.00	11.35	10.21	0.00	7.43	7.19		1.527	1.419
505	107.17	121.5	3.38	11.35	10.21	3.26	7.43	7.19	1.036	1.527	1.419
590	106.32	107.17	0.66	17.63	14.66	0.42	11.19	9.74	1.567	1.575	1.505
504	103	106.32	5.96	17.64	14.66	6.69	11.20	9.74	0.891	1.575	1.505
553	99	103	1.00	19.38	16.57	0.00	12.92	11.23		1.500	1.476
503	98	99	8.78	53.76	67.98	10.52	38.11	49.81	0.835	1.411	1.365
502	82.5	98	19.78	69.81	85.27	19.59	44.71	55.11	1.010	1.561	1.547
501	66.5	82.5	83.01	98.94	111.52	68.58	69.93	69.29	1.210	1.415	1.609

MOMENTS ($x10^3$ Kips feet)

Elem	Elev	Elev	Equivalent static about N-S Axis	Equivalent static about E-W Axis	Time history about N-S Axis	Time history about E-W Axis	Ratio Equivalent static / Time history about N-S Axis	Ratio about E-W Axis
555	163.79	169	2.56	2.34	3.22	2.55	0.793	0.919
508	153	163.79	9.65	9.10	10.91	8.45	0.885	1.077
507	134.25	153	69.39	36.81	54.83	32.80	1.265	1.122
506	134.25	153	47.78	11.37	50.97	14.03	0.937	0.810
554	121.5	134.25	248.46	193.72	183.55	139.00	1.354	1.394
505	107.17	121.5	394.26	355.88	286.60	236.34	1.376	1.506
590	106.32	107.17	432.79	373.39	379.00	256.13	1.142	1.458
504	103	106.32	474.10	431.61	407.28	293.30	1.164	1.472
553	99	103	523.77	507.35	367.88	341.48	1.424	1.486
503	98	99	591.75	561.09	395.94	375.75	1.495	1.493
502	82.5	98	2817.12	2473.33	1780.56	1610.91	1.582	1.535
501	66.5	82.5	8789.52	6960.01	5946.55	5621.72	1.478	1.238

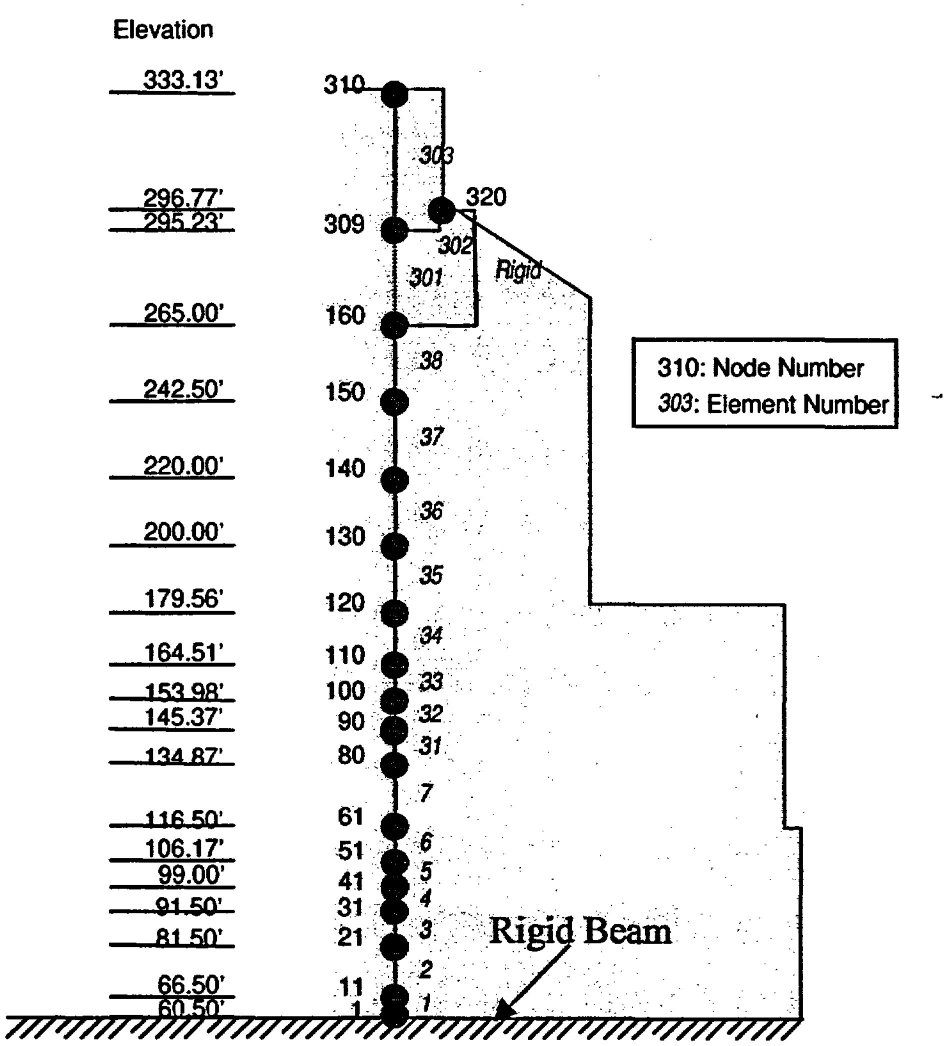

Figure 3.7.2.3-1-1: ASB Stick portion of NI combined model

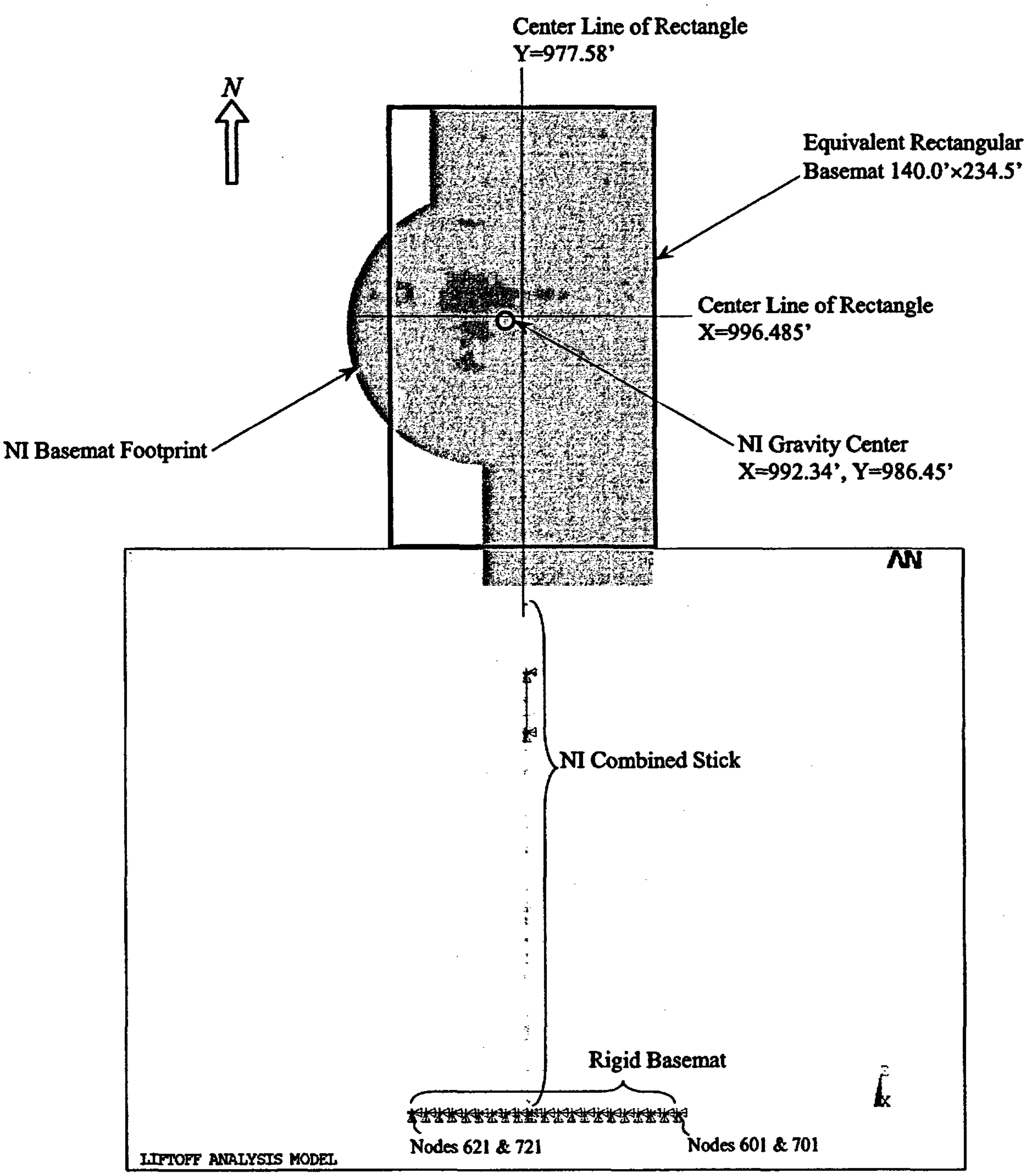

Figure 3.7.2.3-1-2: Rigid Basemat

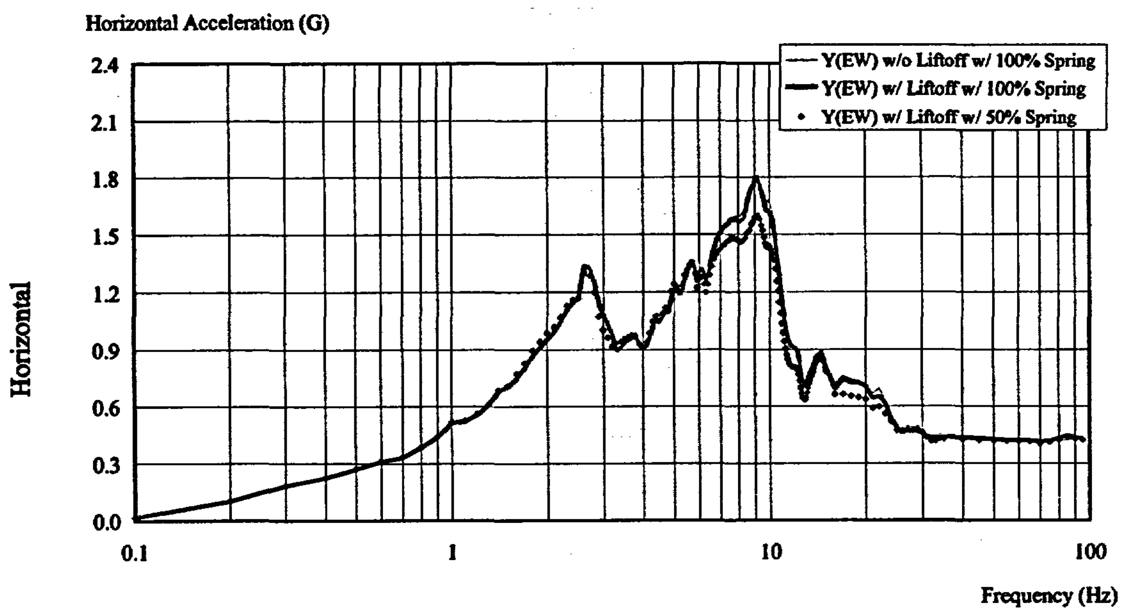

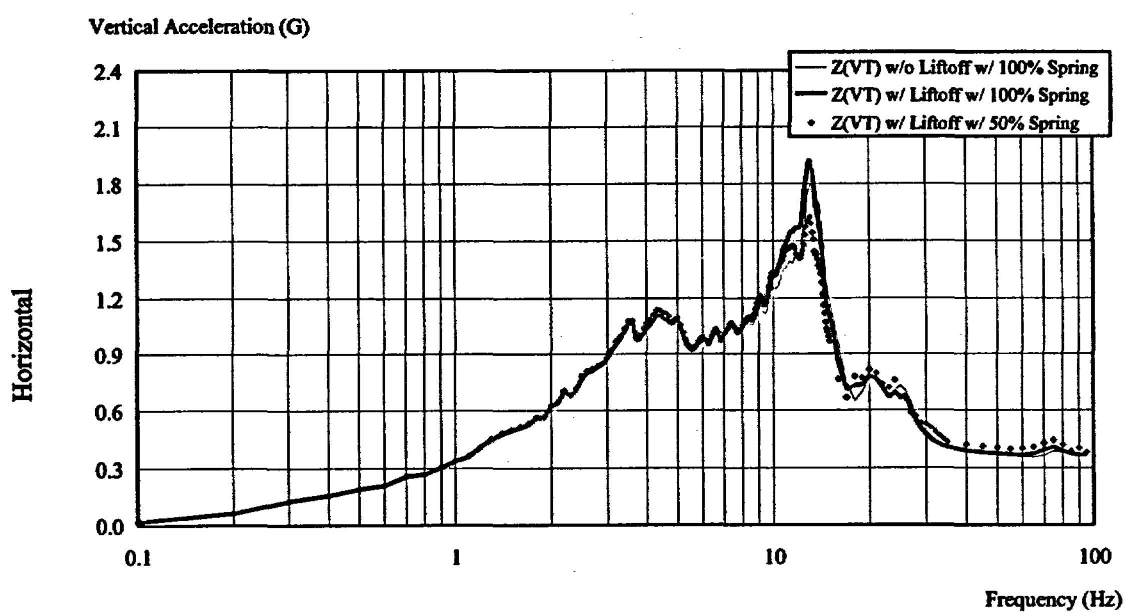

Figure 3.7.2.3-1-3:Floor Response Spectra at 5 % Damping – Node 61 (EL. 116.50')

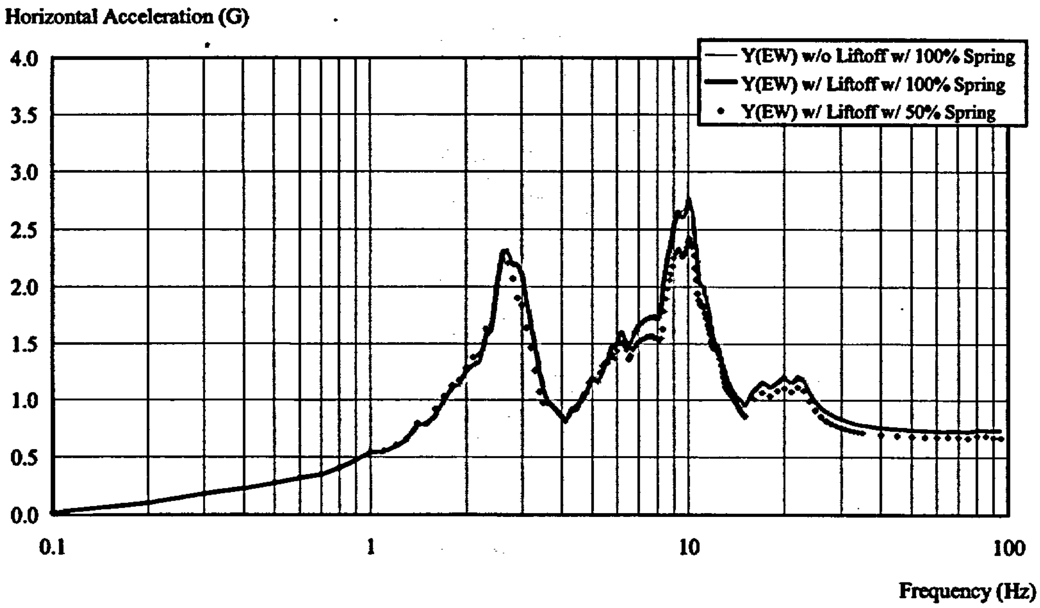

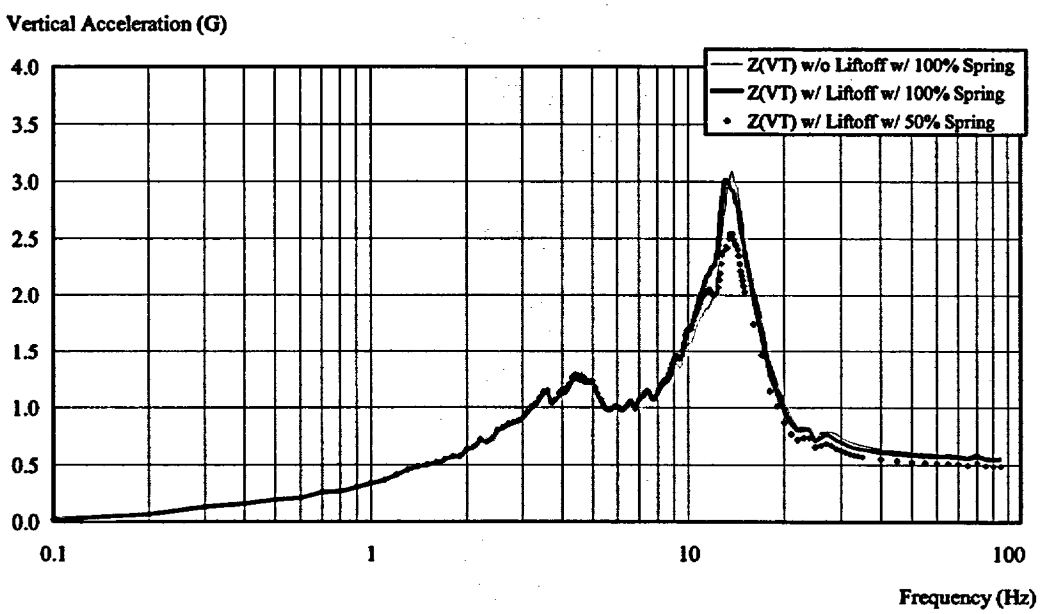

Figure 3.7.2.3-1-4: Floor Response Spectra at 5 % Damping – Node 120 (EL. 179.56')

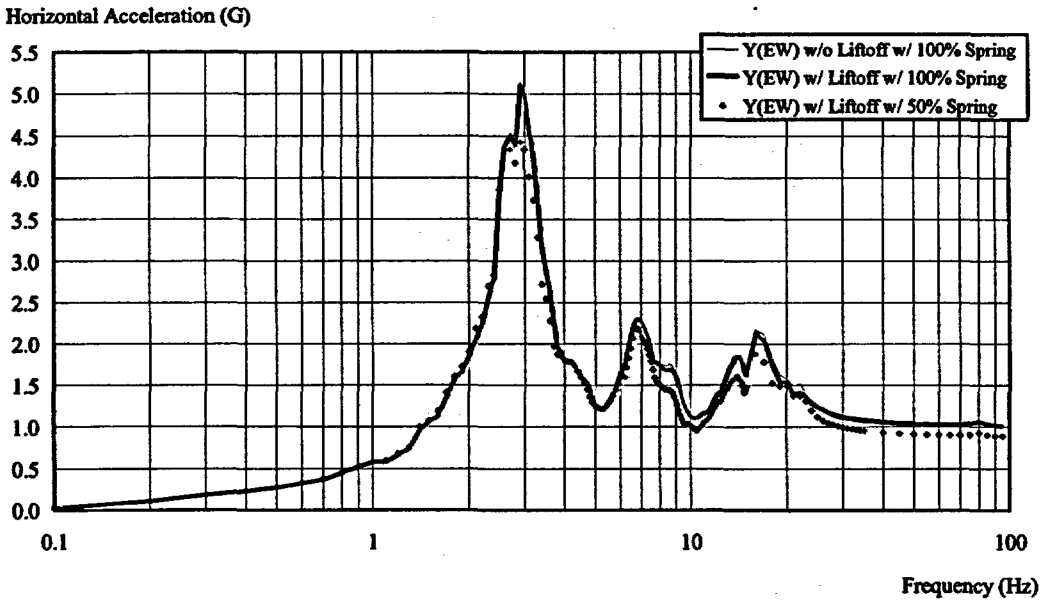

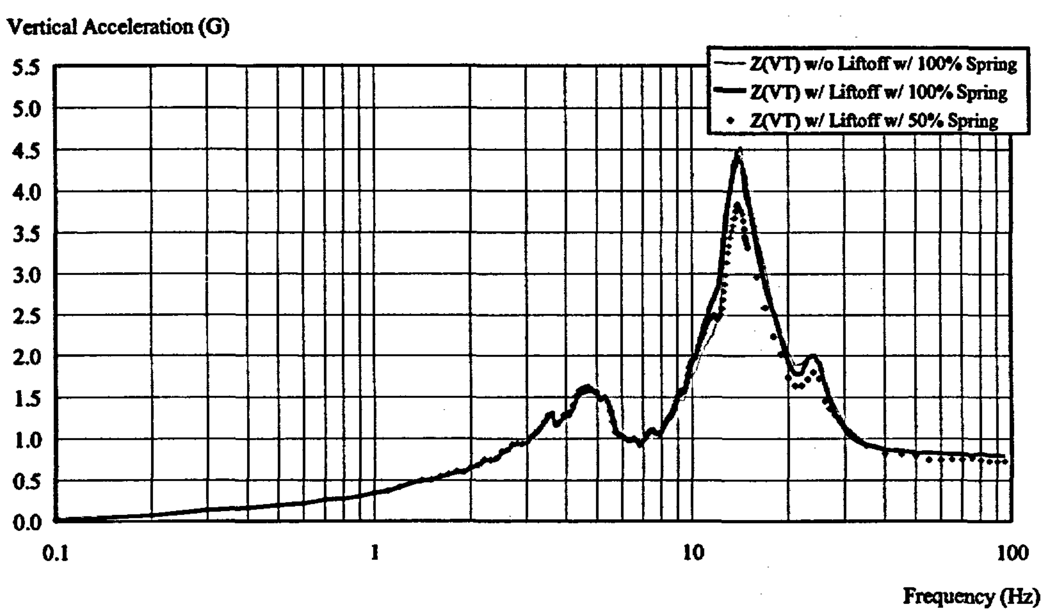

Figure 3.7.2.3-1-5: Floor Response Spectra at 5 % Damping – Node 160 (EL. 265.00')

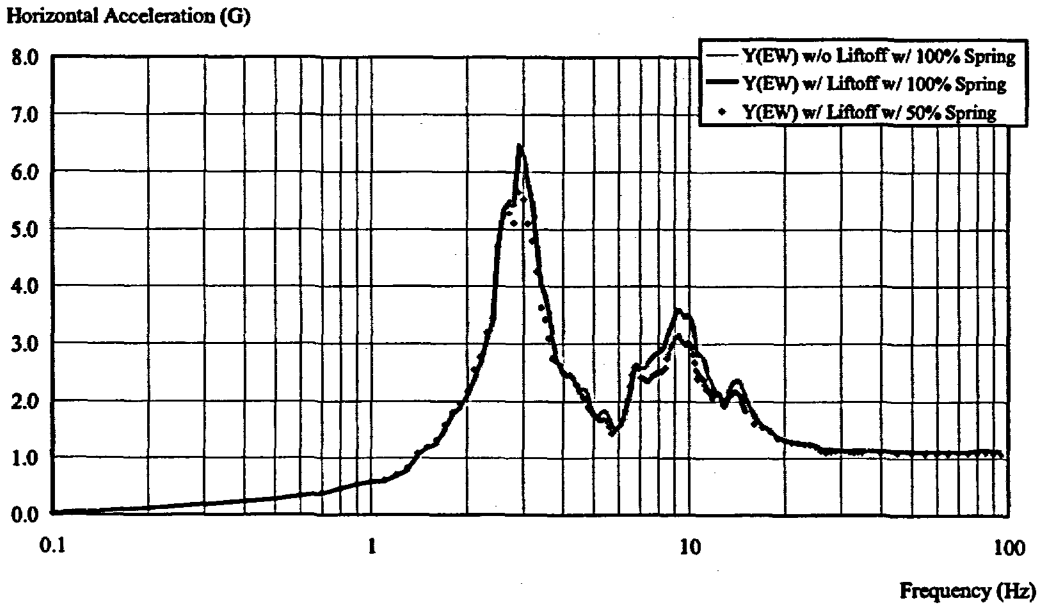

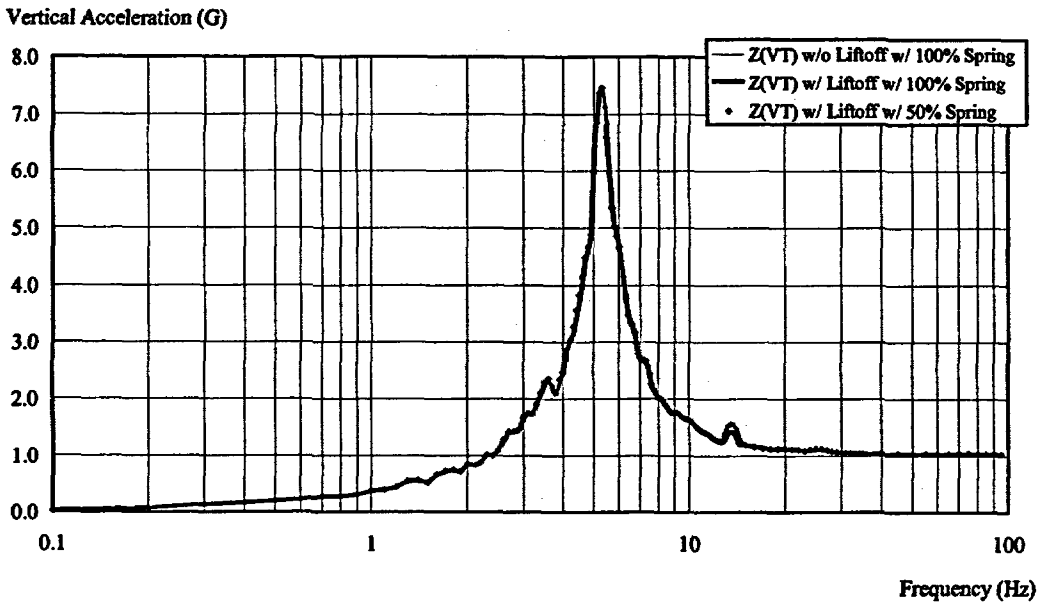

Figure 3.7.2.3-1-6: Floor Response Spectra at 5 % Damping – Node 309 (EL. 295.23')

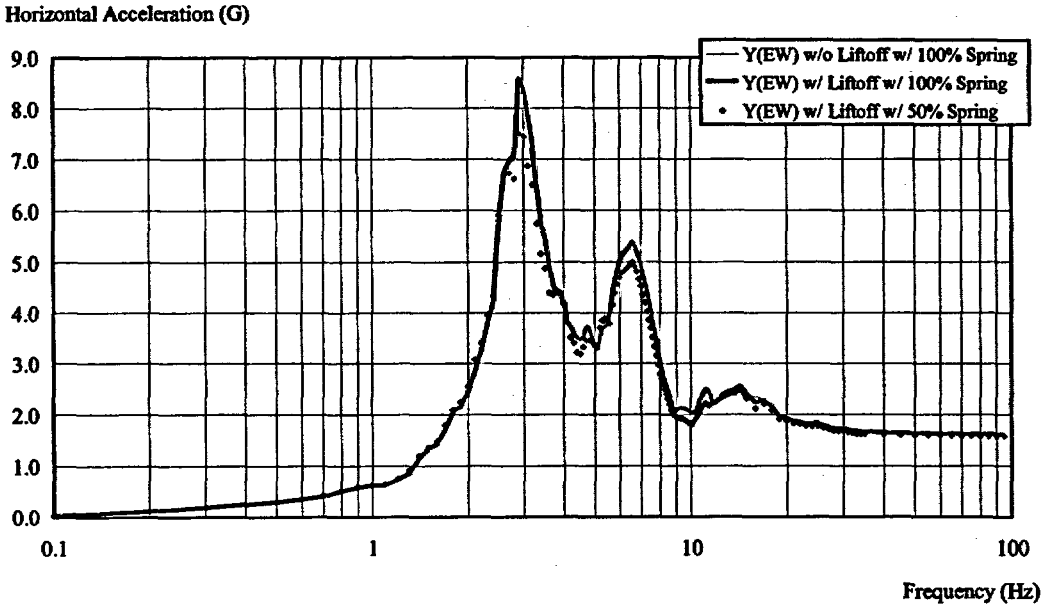

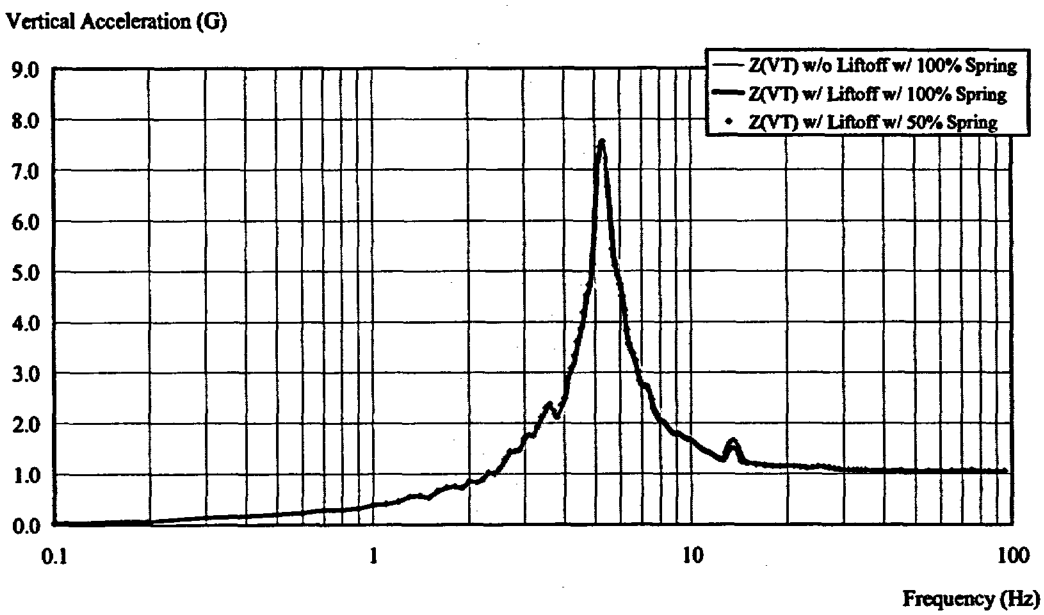

Figure 3.7.2.3-1-7: Floor Response Spectra at 5 % Damping – Node 310 (EL. 333.13')

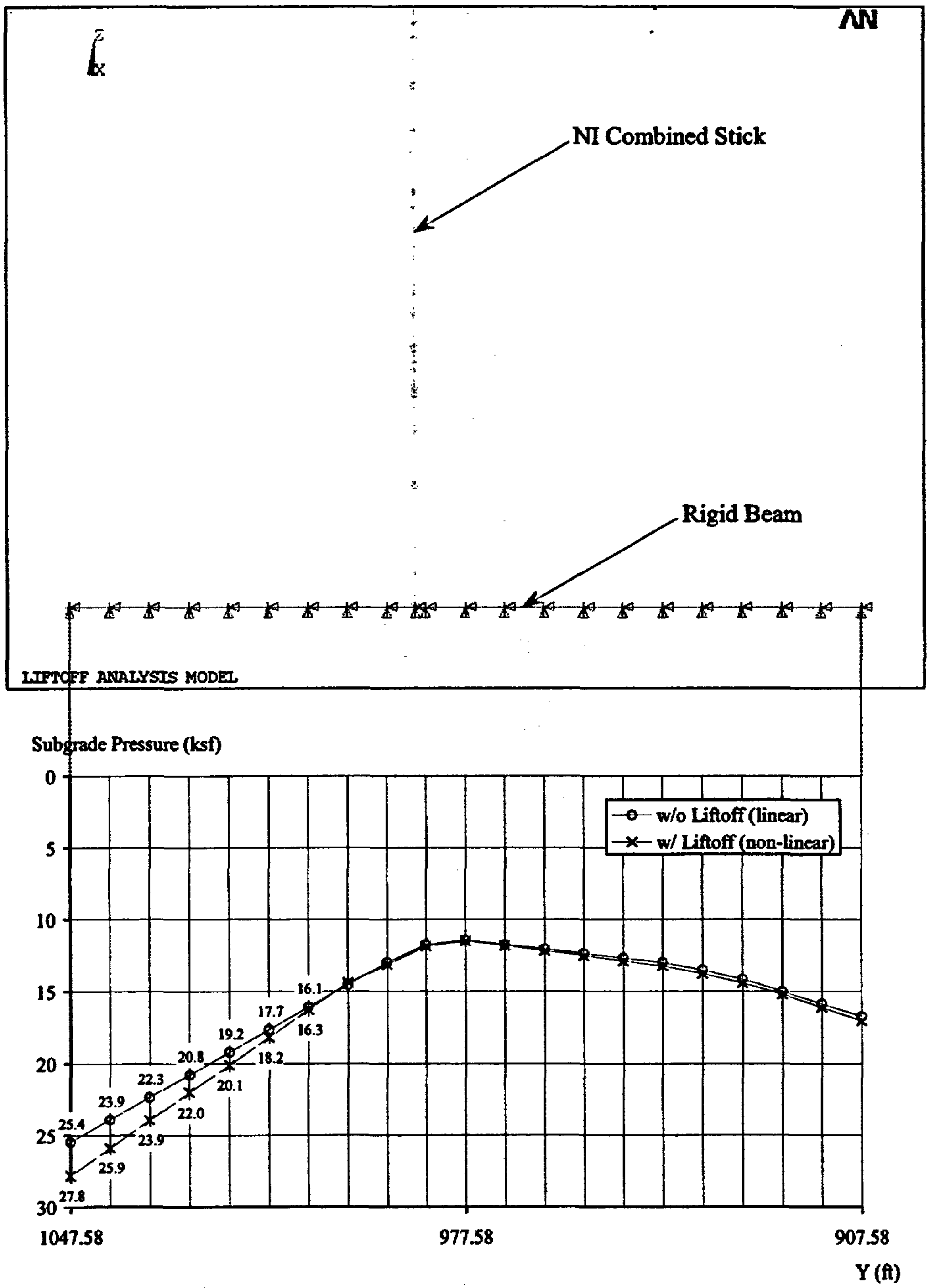

Figure 3.7.2.3-1-8: Maximum Dynamic Subgrade Pressure Distribution

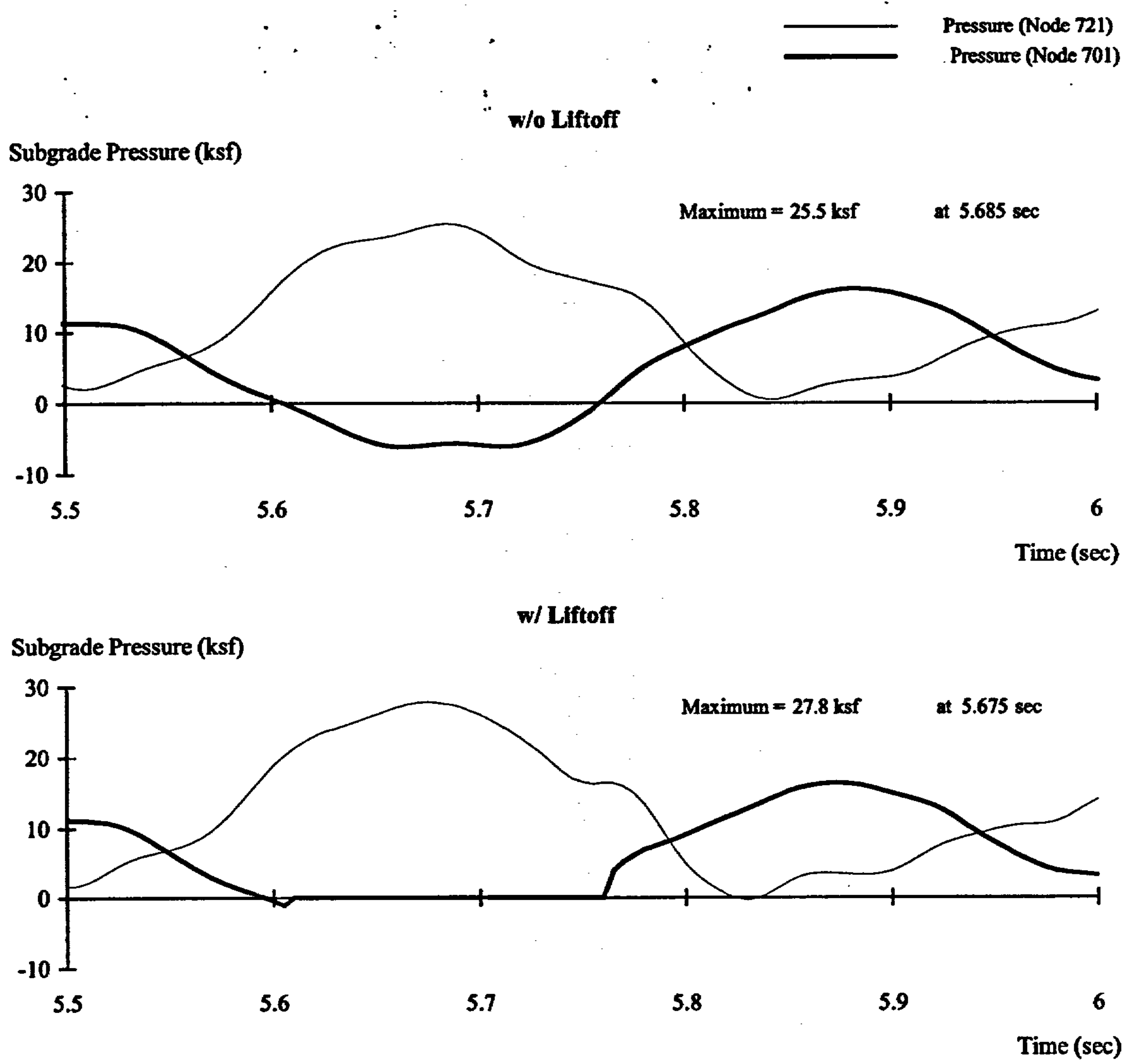

Figure 3.7.2.3-1-9: Time History of Basemat Edge Pressure

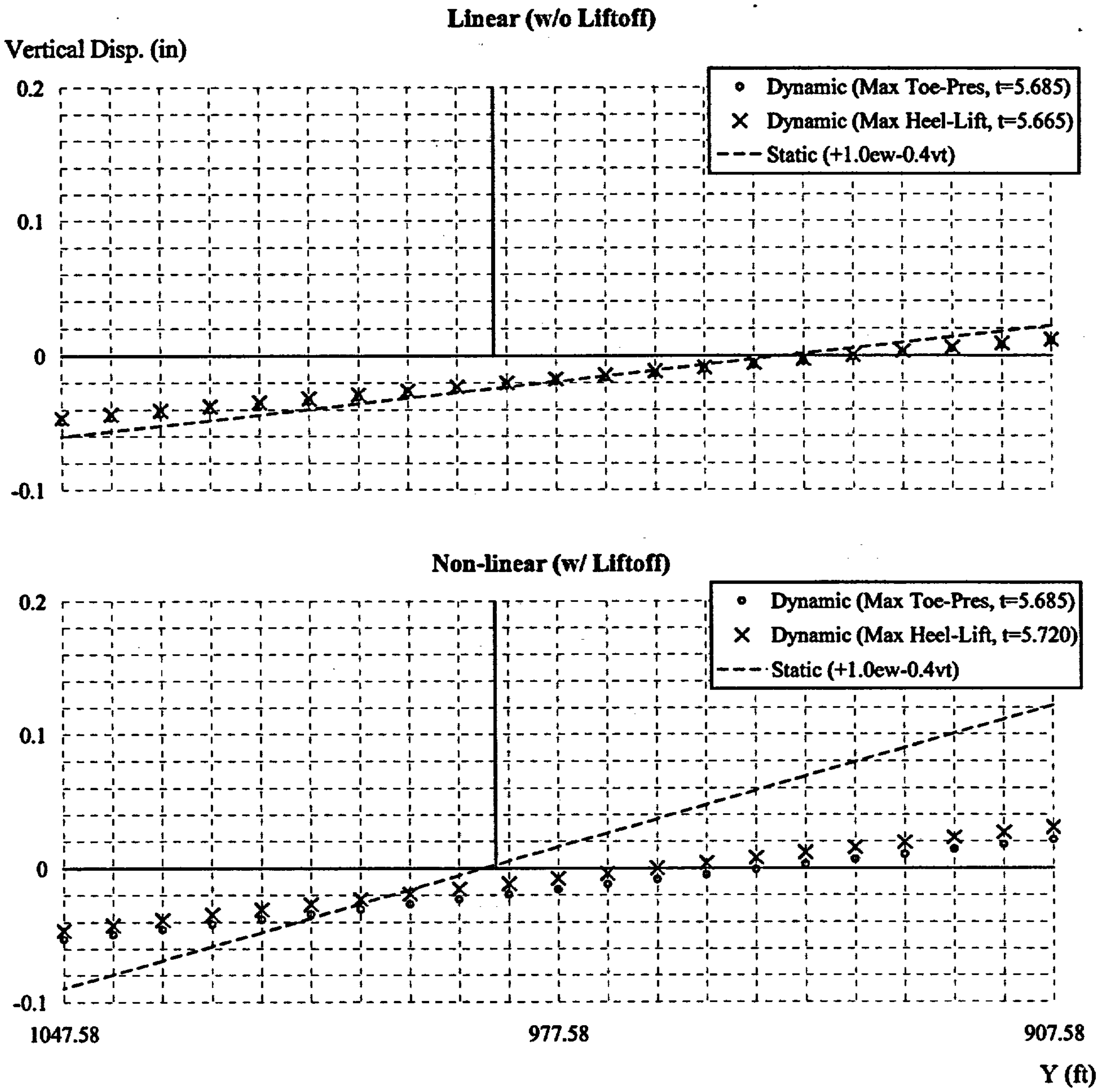

Figure 3.7.2.3-1-10: Basemat Displacements

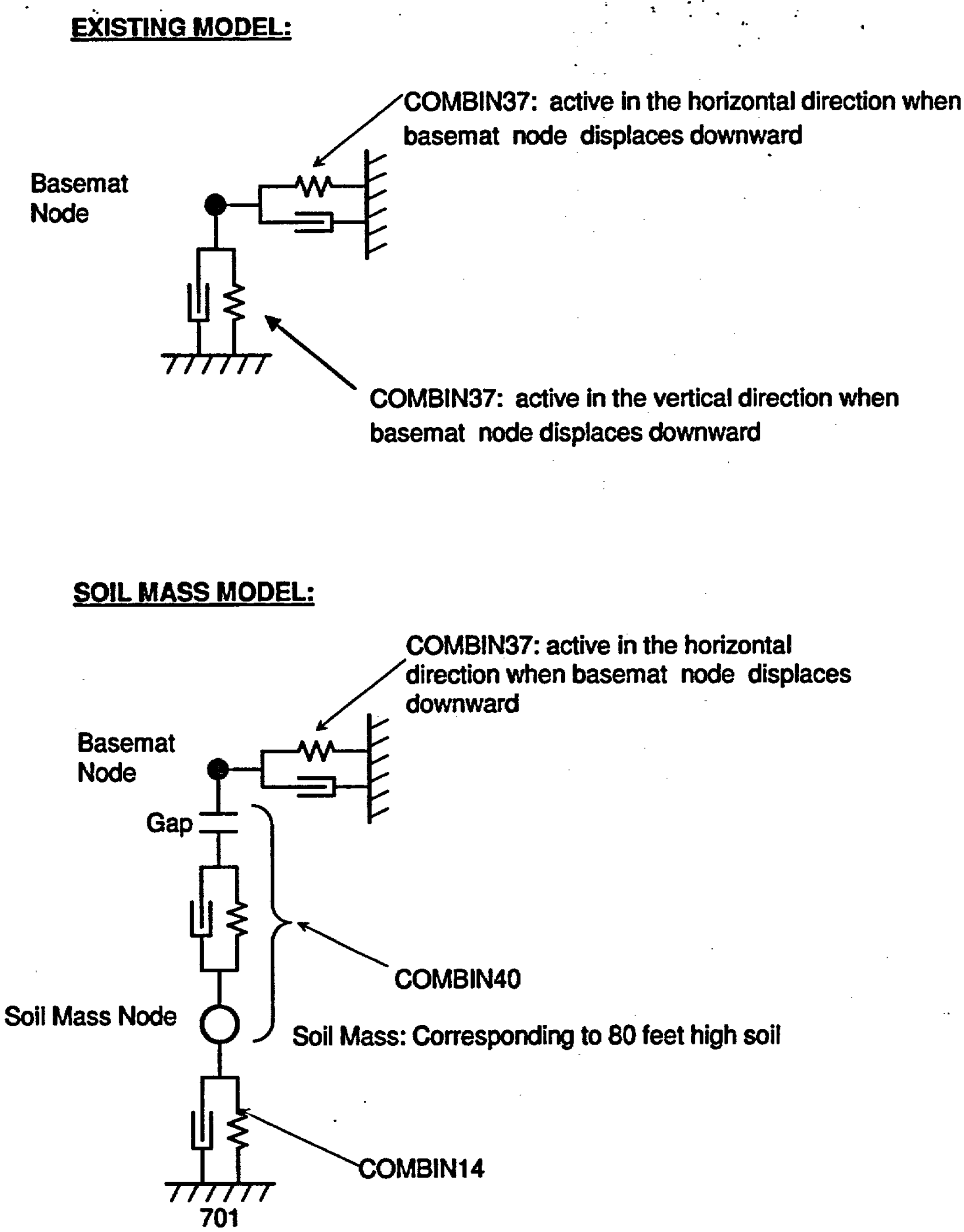

FIGURE 3.7.2.3-1-11: ADDING SOIL MASS ELEMENT

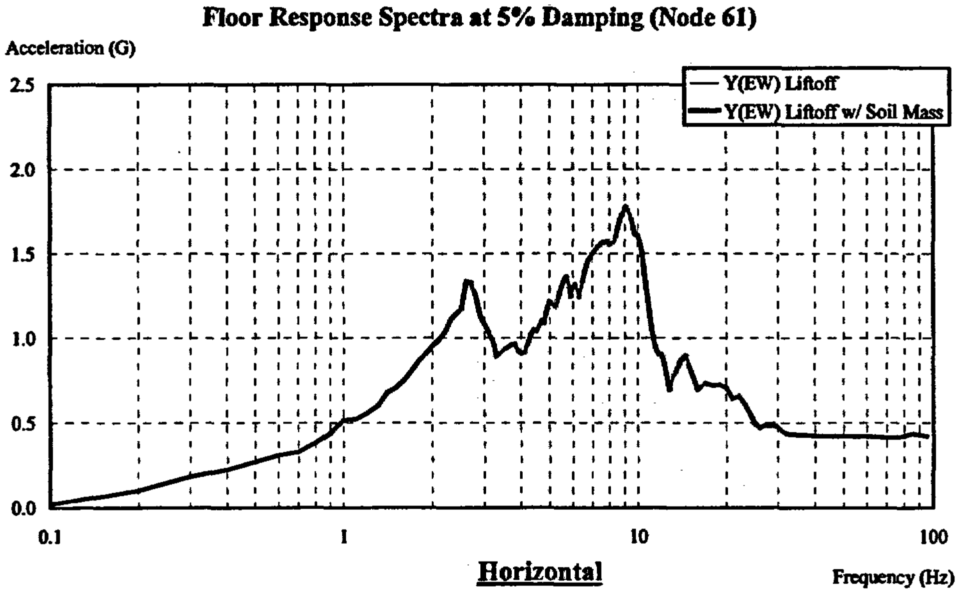

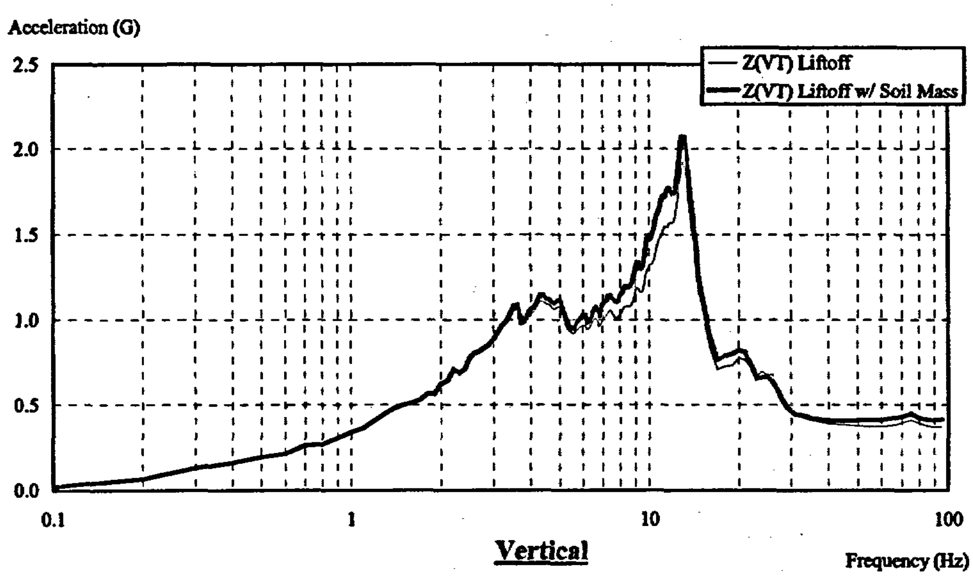

FIGURE 3.7.2.3-1-12: FRS – ASB EL. 116.50', 0.3G SSE

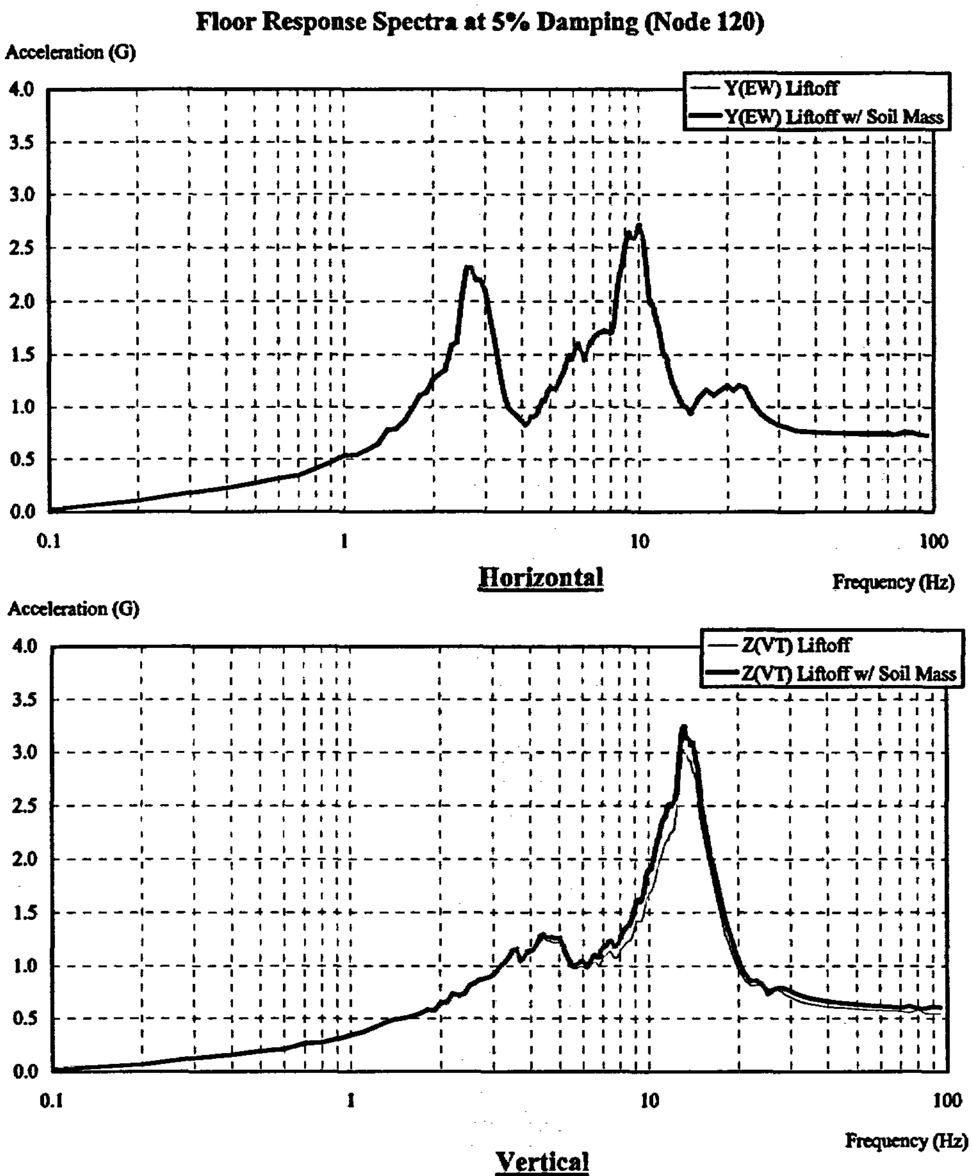

FIGURE 3.7.2.3-1-13: FRS – ASB EL. 179.56', 0.3G SSE

Floor Response Spectra at 5% Damping (Node 160)

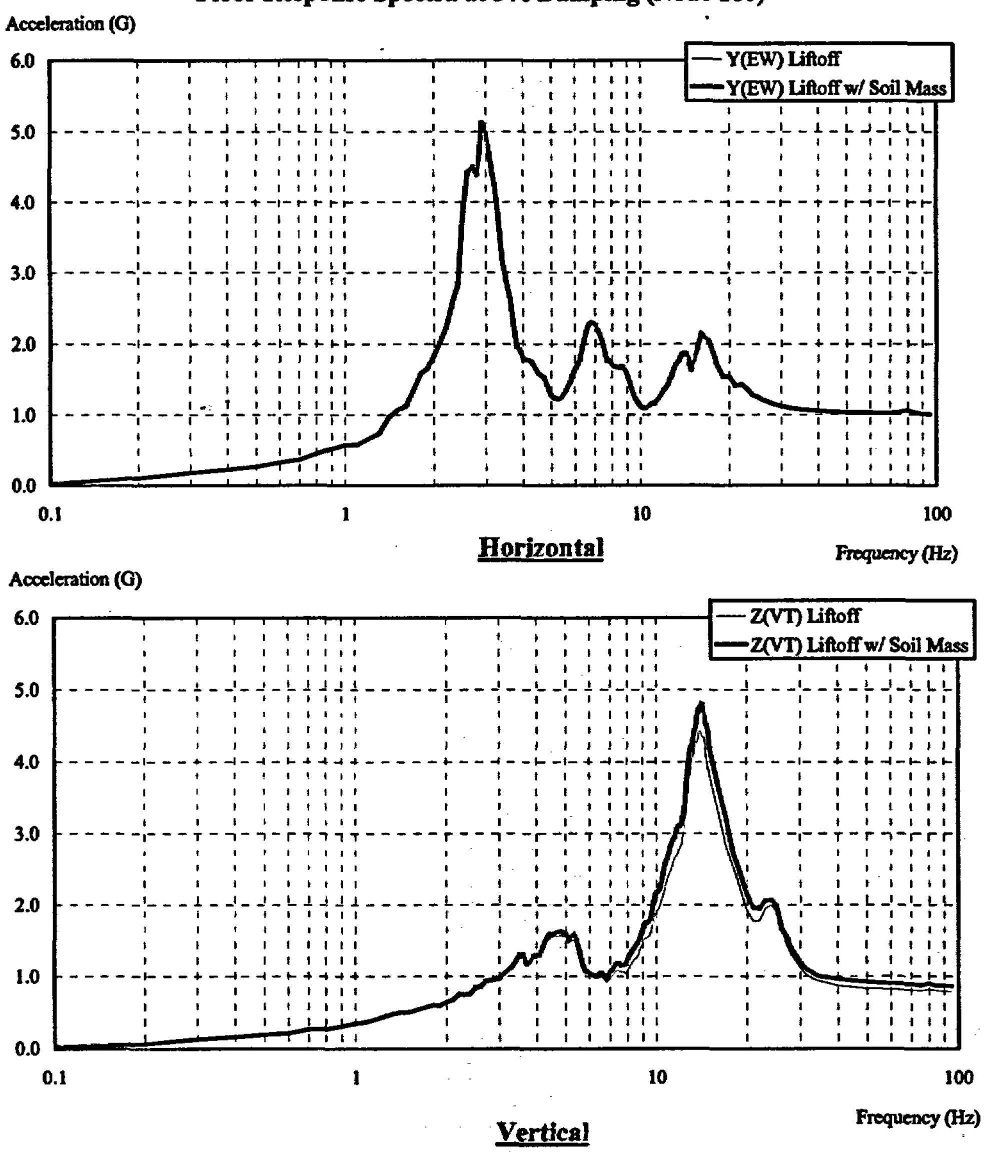

FIGURE 3.7.2.3-1-14: FRS – ASB EL. 265.00', 0.3G SSE

Floor Response Spectra at 5% Damping (Node 309)

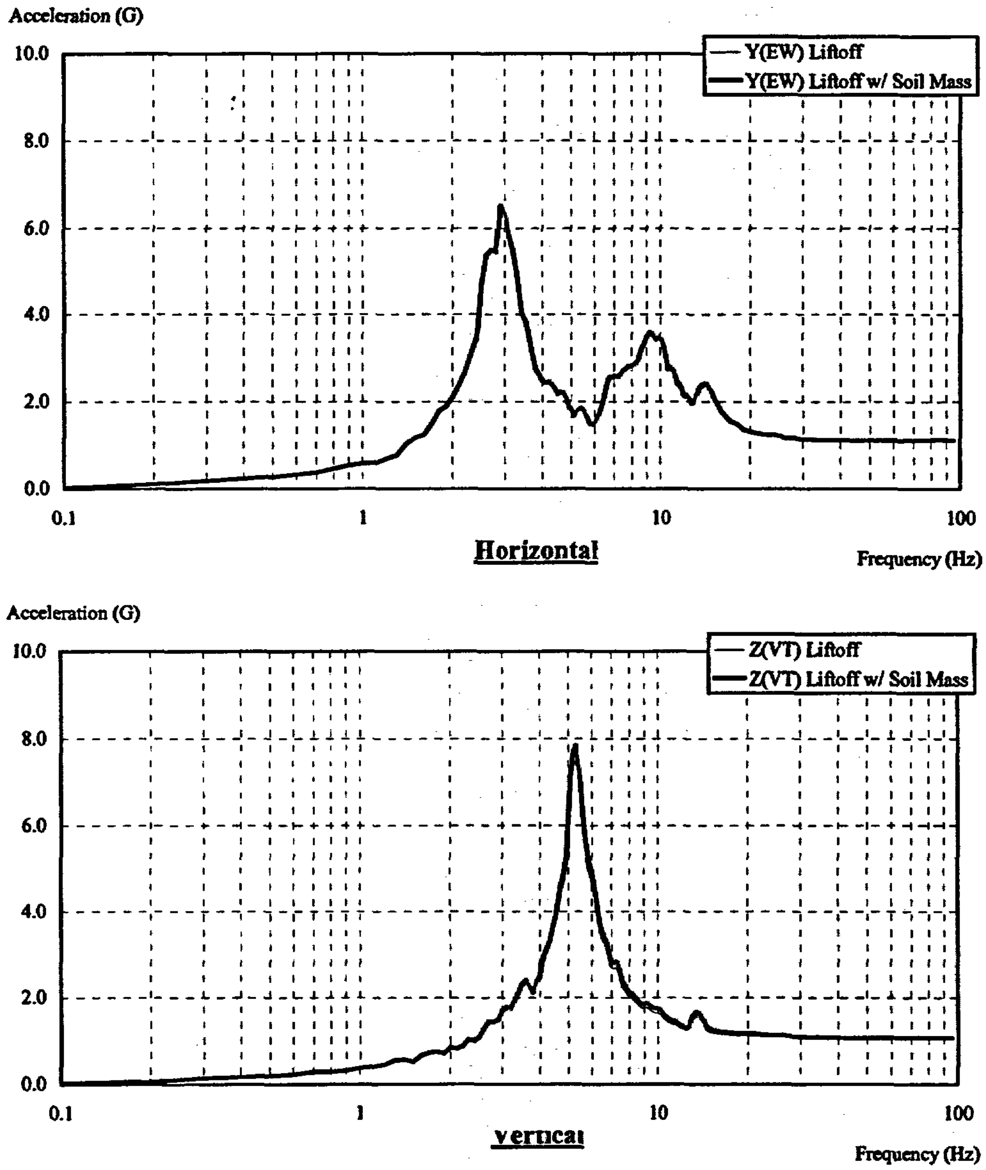

FIGURE 3.7.2.3-1-15: FRS – ASB EL. 295.23', 0.3G SSE

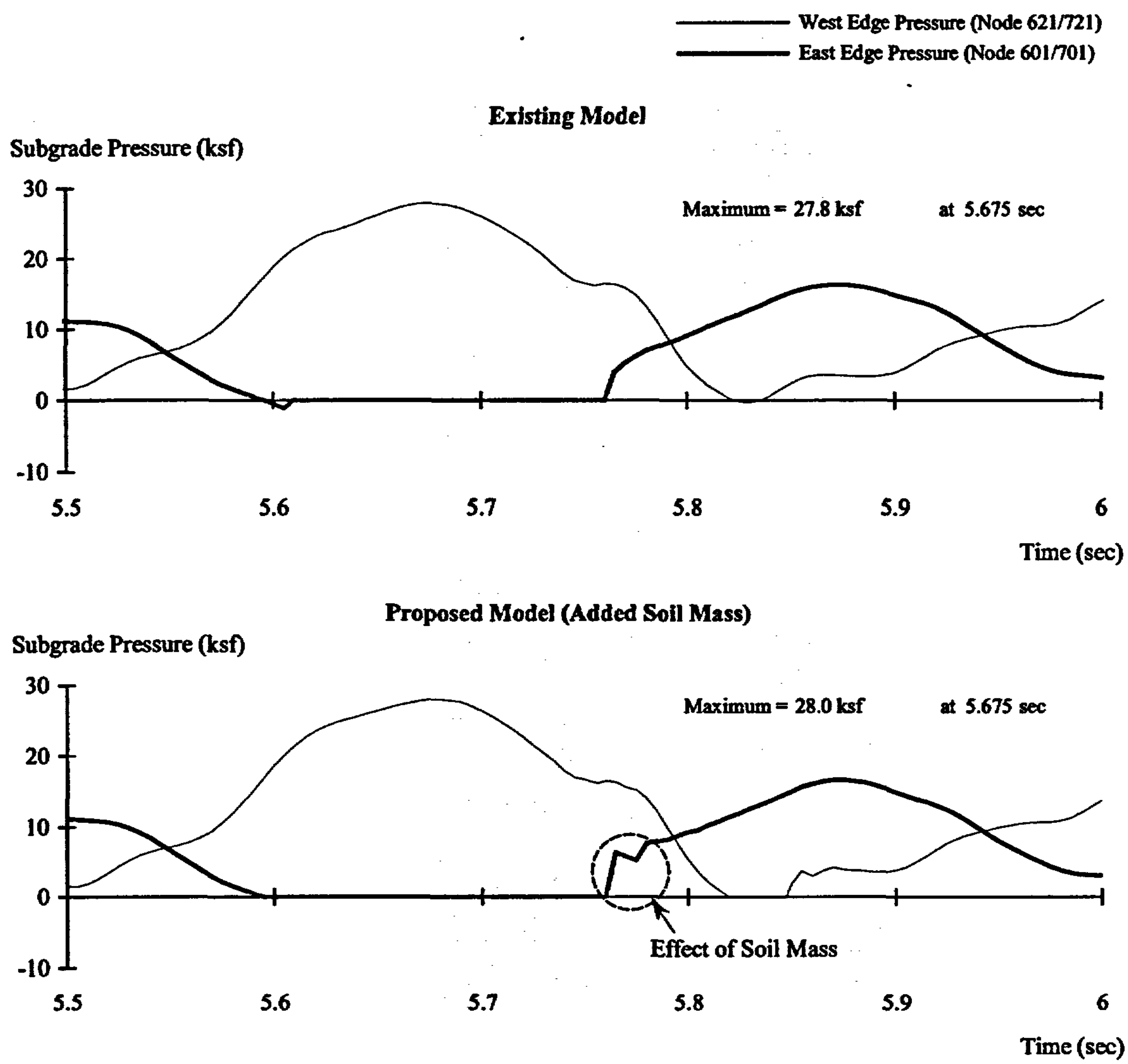

FIGURE 3.7.2.3-1-22: TIME HISTORY OF BASEMAT EDGE PRESSURES (0.3G SSE)

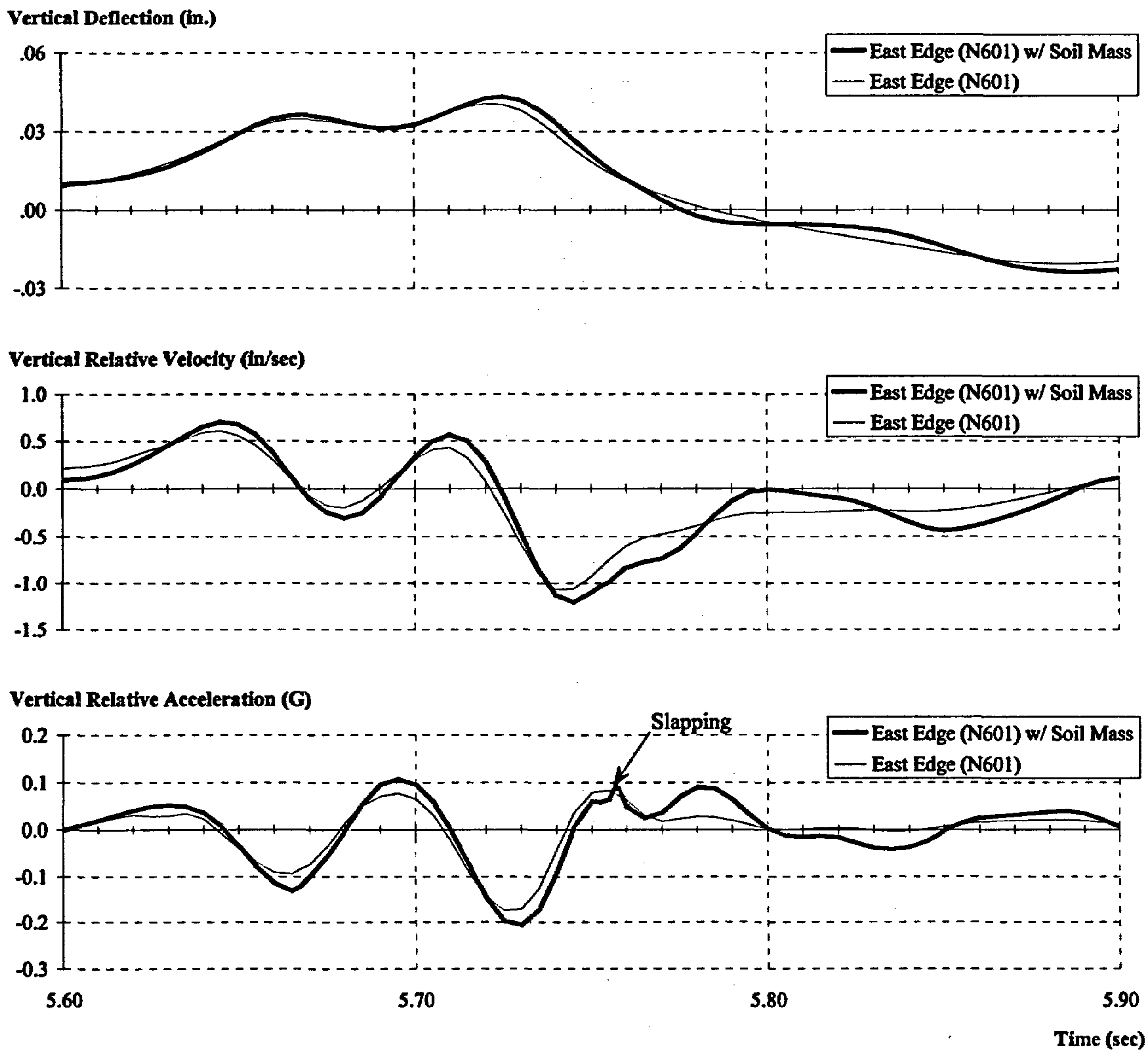

FIGURE 3.7.2.3-1-24: TIME HISTORY OF HEEL EDGE AROUND SLAPPING (0.3G SSE)

AP1000 DESIGN CERTIFICATION REVIEW

Draft Safety Evaluation Report Open Item Response

DSER Open Item Number: 3.8.5.4-1 (Revision 1)

Original RAI Number(s): 230.022

Summary of Issue:

In its review of DCD Tier 2 Section 3.8.5.4, the staff determined that the potential uplift and slapping back of the containment internal structures foundation on the basemat through the steel containment vessel during a seismic event could affect both the seismic design loads and in structure response spectra for all structures, systems and components associated with the containment internal structure, and could also affect the seismic response of the steel containment shell. In RAI 220.021, the staff requested the applicant to perform additional analyses to demonstrate how the uplifting effect will be addressed, and how the uplifting effect on the seismic analysis results will be used for the design of the containment and containment internal structures. This is Open Item 3.8.5.4-1.

Westinghouse Response (Revision 1):

The bottom head of the containment vessel rests on the nuclear island basemat. The containment internal structures basemat rest within the bottom head. There are no shear studs or anchors designed to transfer loads tangential to the vessel surface. The interface is designed to transfer load in compression and friction. The configuration is identical to the AP600 and the stability evaluation shown in Figure 3.8.5.4-1-1 follows the AP600 methodology described in the AP600 response to RAI 230.47.

The provisions in the nuclear island basemat model are included for use in the equivalent static analyses to develop design loads for basemat design. The uplift capability assures that the reaction between the two basemats is correctly transferred as compression loads only. The stability evaluation shows a factor of safety against overturning of about 2.1. Since the deadweight has not been overcome, no "liftoff or slapping" is expected to occur. However, allowing for a small separation of the containment internal structures from the basemat, there would be no significant effect to the seismic design loads or the in-structure response spectra. A small separation (slapping) might cause small localized changes in seismic response loads similar to those for the lift off observed between the nuclear island basemat and the rock addressed in the response to DSER Open Item 3.7.2.3-1. Any change in high frequency response due to "slapping back" would not propagate through the building structures to affect the seismic response. This is because of energy loss, damping, and filtering effects due to gaps and cracking. Therefore, it is not necessary to modify the analysis methods from those that were accepted by the NRC for the AP600 plant.

To support the conclusions established by the hand calculation, alternate non-linear analyses were performed using ANSYS. As shown in Figure 3.8.5.4-1-2, the analysis model consists of the following three components:

1) A superelement of the containment internal structures
2) Boundary nodes used to define the interface between the containment vessel and the Nuclear Island base-mat
3) Contact elements that represent compression and friction.

The steel containment vessel (SCV) weighs less and has a higher center of gravity than the CIS. Initially, its overturning will be resisted by its own weight and the weight of the CIS. Thus, the SCV will uplift together with the CIS. For this reason, the SCV is not modeled explicitly, but instead the SCV overturning is represented using steel containment vessel and polar crane loads, applied as concentric forces on the CIS super-element boundary nodes at elevation 100'.

Overturning and sliding analyses were performed using DL + SSE loads. The SSE loads were applied as equivalent static loads using the 100-40-40 rule. The loads were gradually increased from zero using increments of 0.05 SSE until instability occurred (about when the load reached 1.8 times the SSE load, Alpha=1.8). The vertical seismic load was applied in the direction opposite to the dead weight, and the horizontal seismic load was applied from the center of containment to the center of mass of the containment internal structures to minimize the dead load resistance.

Results for the DL combined with SSE where the EW seismic is the predominant load (-0.4NS + 1.0EW +1.0VT) are shown in Figures 3.8.5.4-1-3 and 3.8.5.4-1-4. Cases where either NS or VT SSE are the predominant loads were also analyzed and show similar results. Figure 3.8.5.4-1-3 shows the vertical displacement at the edge of the containment internal structures where lift-off is maximum. Figure 3.8.5.4-1-4 shows the normal bearing reaction and the sliding reaction at the location of the maximum bearing reaction.

The ANSYS results confirm the hand calculation conclusions, the separation between containment internal structures and the basemat during a seismic event is small, and thus would not have a significant effect on the seismic design loads or the in-structure response spectra.

Design Control Document (DCD) Revision:

None

PRA Revision:

None

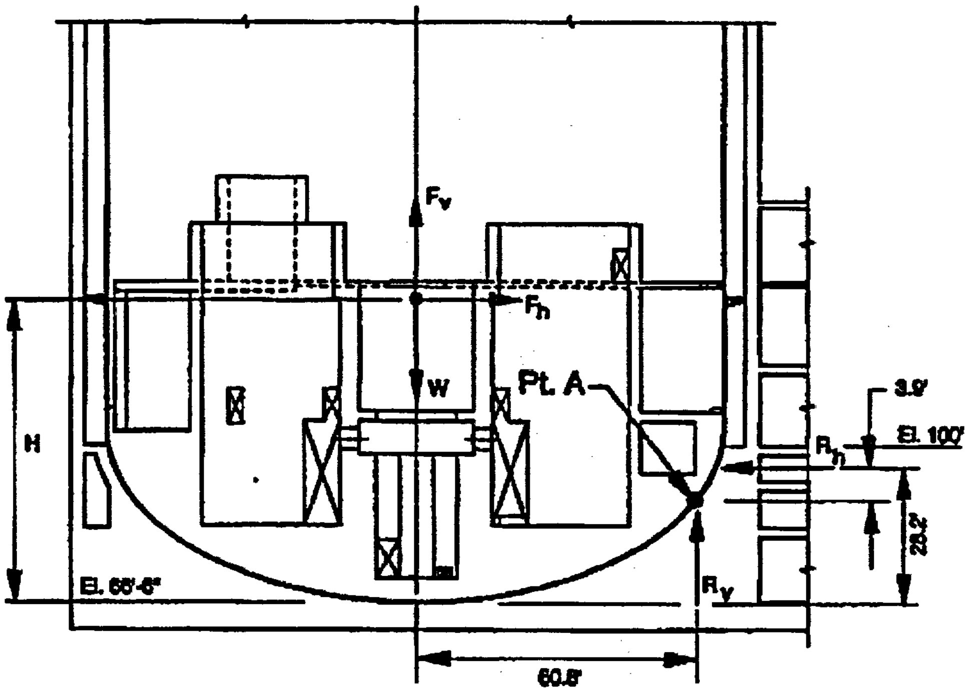

Figure 3.8.5.4-1-1
Free-body Diagram for Containment Internal Structures Overturning Evaluation

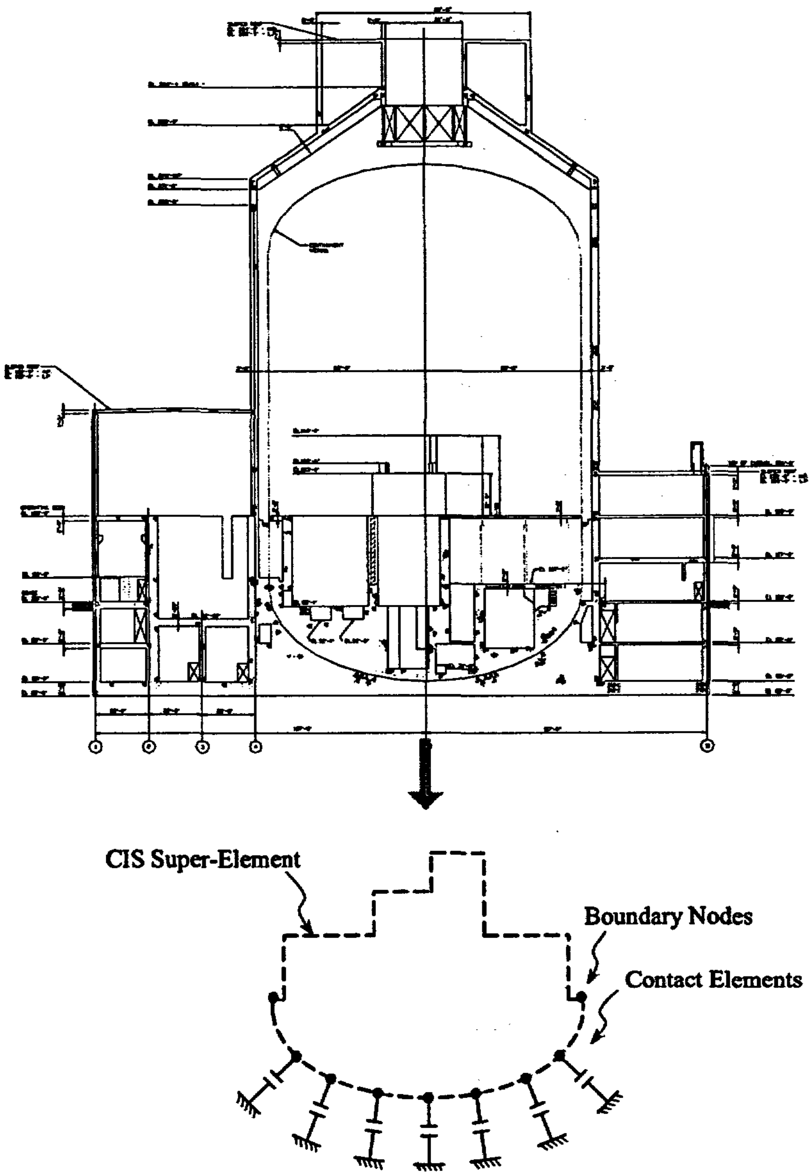

Figure 3.8.5.4-1-2
Free-body Diagram for Containment Internal Structures Overturning Evaluation

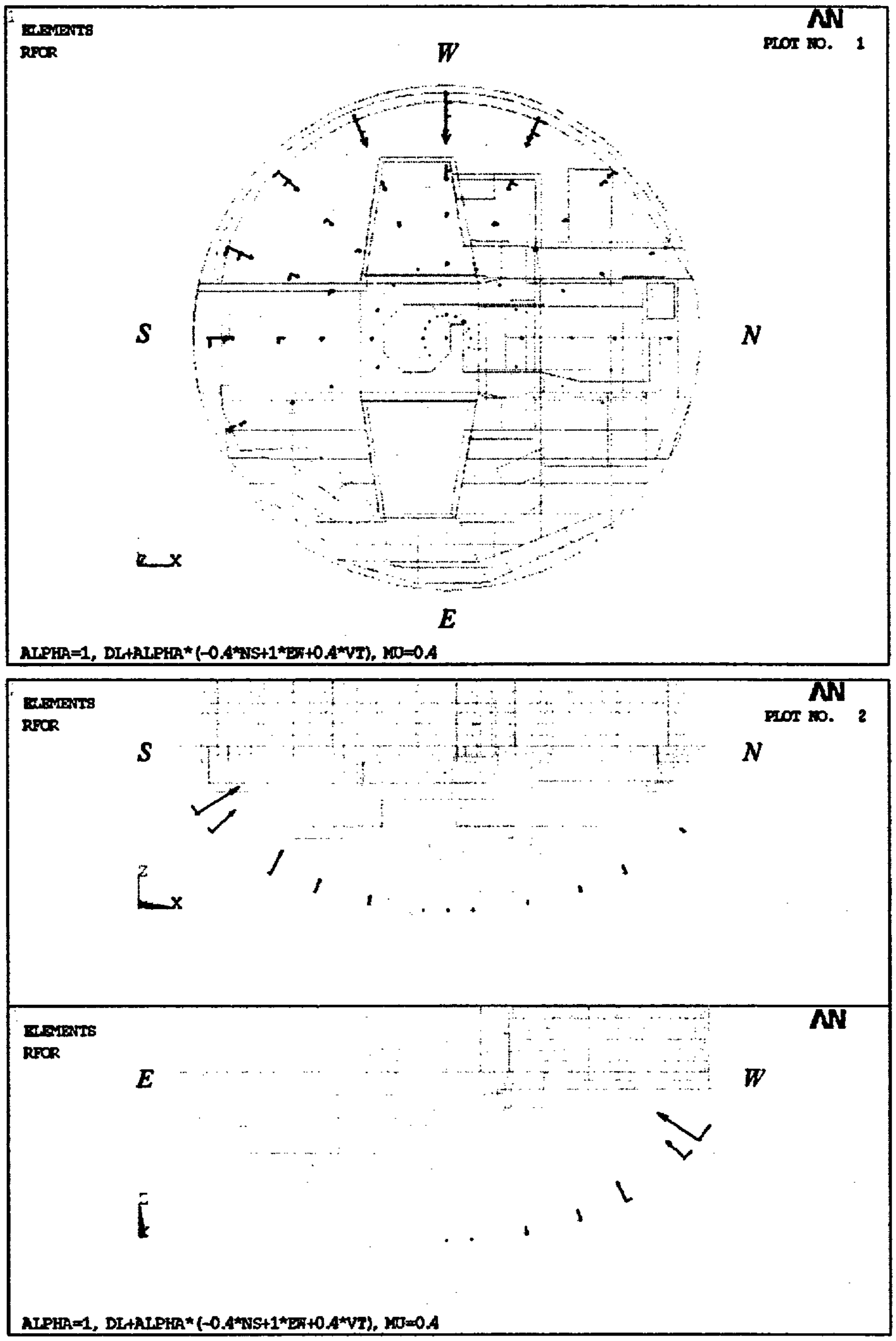

Figure 3.8.5.4-1-3
Reaction Forces for DL + SSE (EW being the predominant load, Alpha=1.0)

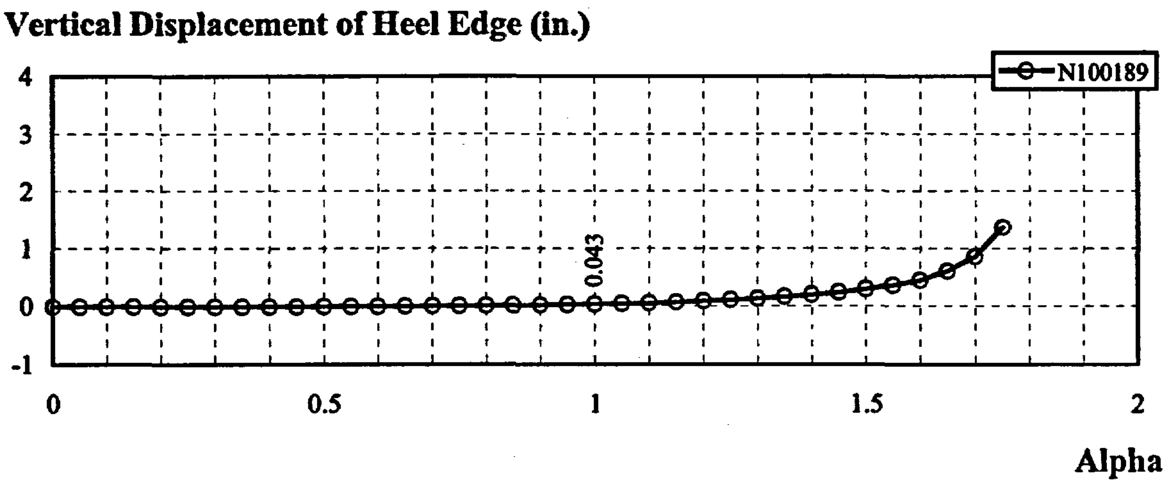

DL+Alpha*(-0.4NS+1.0EW+0.4VT), Mu=0.4

A=138.7 sq.ft

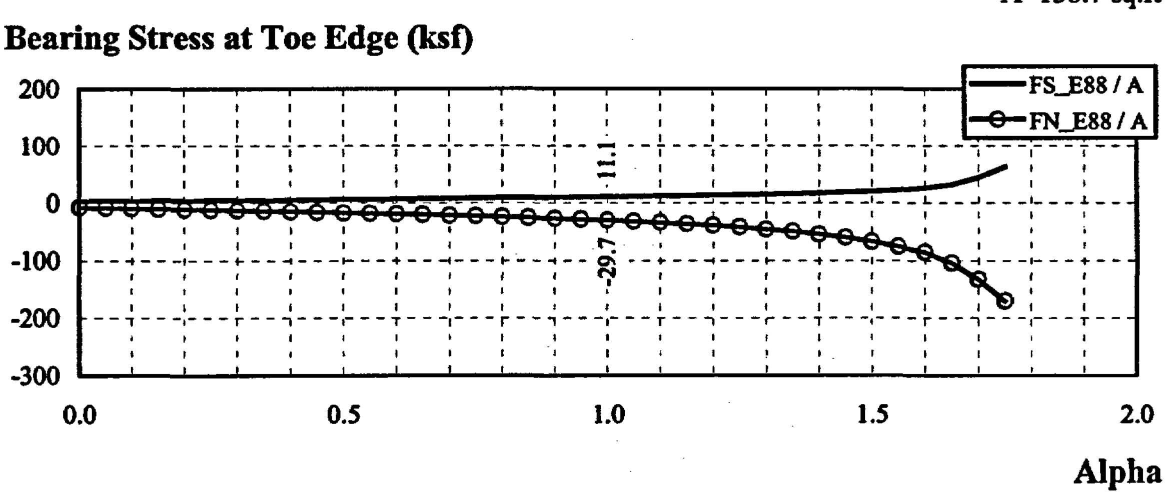

Figure 3.8.5.4-1-4
Vertical Heel Displacements and Toe Bearing Pressures for DL + SSE (EW being the predominant load, Alpha=1.0)

DSER Open Item Number: 4.5.2-1

Original RAI Number(s): None

Summary of Issue:

The core shroud is a welded assembly using cold worked 316L stainless steel. Given the increasing amount of light water reactor experience, will this component be immune to stress corrosion cracking, especially since the fast neutron flux will be increased over current designs? Discuss the impact of this potential aging effect on the integrity of the reactor core shroud, including the effect under accident scenarios. What inspections, if any, in addition to those required by the American Society of Mechanical Engineers (ASME) Code, will be performed by AP1000 combined license (COL) holders to detect these aging effects?

Westinghouse Response:

The YGN-5 core shroud, which is similar to the AP1000 core shroud, is a welded assembly. The starting material is hot rolled, annealed and pickled Type 304 SS procured to SA240. The shroud plates (panels) are cold formed to produce the desired shapes. After the plates are formed, the ribs are welded on and the assembly straightened. The forming and straightening produce areas (specifically the corners) where the austenitic stainless steel is in a cold-worked condition. Most of the shroud remains in the annealed condition. Depending on the neutron fluence, stressed areas of the core shroud may be susceptible to different types of stress corrosion cracking (SCC). Below a neutron fluence of approximately 10^{21} n/cm^2 the stressed area could be susceptible to intergranular or transgranular SCC. The threshold fluence for irradiation assisted stress corrosion cracking (IASCC) is in the range of 2×10^{21} to 1×10^{22} n/cm^2.

Transgranular stress corrosion cracking (TGSCC) occurs when austenitic stainless steels are highly stressed and exposed to high temperature water containing a significant amount of dissolved oxygen and some level of chlorides. There have been numerous events of TGSCC in PWR applications. In all cases, the cracking occurred in stagnant flow regions where high levels of dissolved oxygen could form during outages and could persist upon return to service. The core shroud will be exposed to the flowing core coolant. The dissolved oxygen level of the flowing coolant in PWRs is very low and chloride levels in the primary coolant are controlled to low levels. Further, there are no crevice regions in the core shroud where stagnant conditions could exist. Hence, TGSCC in the core shroud is very unlikely.

In PWR applications, there have been few occurrences of intergranular stress corrosion cracking (IGSCC). Laboratory testing and field experience indicate IGSCC typically occurs in austenitic stainless steels with sensitized microstructures that are highly stressed in high temperature water containing significant levels of dissolved oxygen. In PWRs, the dissolved oxygen levels are maintained at very low levels (typically less than 2 ppb) by the addition of hydrazine (an efficient oxygen scavenger at temperatures above 150°F) during plant start-ups and by maintenance of a hydrogen over pressure during operation to reduce oxygen resulting from radiolytic decomposition of water. In addition to the primary coolant chemistry controls, additional features during core shroud fabrication will provide further assurances that IGSCC will be an unlikely event. These features include use of annealed Type 304 SS as the starting material for core shroud fabrication, reduced carbon levels, and control of heat input during welding. The latter two minimize the potential for sensitization of the Type 304 SS during fabrication. Also, cleaning materials and consumable materials used during fabrication are controlled to ensure that Type 304 SS surfaces are not contaminated during fabrication with materials that could lead to IGSCC. The fabrication features and the operational controls in the areas of RCS chemistry will ensure that IGSCC is a low potential event during the AP1000 lifetime.

Irradiation assisted stress corrosion cracking (IASCC) can occur in austenitic SS after long term exposure to high levels of neutron irradiation. IASCC has been common in BWRs where the combination of relatively high neutron fluences and more aggressive (than PWRs) environmental conditions (specifically, relatively high oxygen levels) have resulted in IASCC of reactor vessel internals. IASCC has occurred only infrequently in PWR applications, with the only significant occurrences being in highly stressed, cold-worked Type 316 baffle former bolts in several French PWRs. These failures have been used to estimate threshold fluences for IASCC in PWR applications.

The core shroud panels will be the most limiting parts of the reactor vessel internals with respect to cumulative neutron fluence. Some areas of the core shroud may have maximum fluences that are in the threshold fluence range for IASCC. However, the potential for IASCC in the core shroud panels is mitigated by several factors, including the use of annealed starting material. The most important factor relative to potential for IASCC is the water chemistry conditions at the locations of highest stresses. The core shroud panels are exposed to the primary coolant environment that has low dissolved oxygen levels as discussed above. Because of the welded configuration, there are no crevice regions, such as those between bolts and core shroud components, where relatively high levels of dissolved oxygen could develop and persist. With the low oxygen levels, IASCC is an unlikely degradation mechanism.

In summary, SCC and IASCC are unlikely in the AP1000 core shroud because of the material used for fabrication and the environmental conditions, specifically the low oxygen levels, which will be present in the high stressed regions of the shroud.

Based on the successful operation of current plants with core shrouds, no additional inspections of the reactor internals beyond the refueling outage and ten-year interval visual inspections specified by American Society of Mechanical Engineers (ASME) Code Section XI are expected to be required by AP1000 combined license (COL) holders. Development of the plant specific in-service inspection program is the responsibility of the Combined License (COL) holder.

Design Control Document (DCD) Revision:

None

PRA Revision:

None

AP1000 DESIGN CERTIFICATION REVIEW

Draft Safety Evaluation Report Open Item Response

DSER Open Item Number: 6.1-1

Original RAI Number(s):

Summary of Issue:

The design of the shear section of the automatic depressurization system - stage 4 (ADS-4) squib valve may be creating a situation where there is a severe design notch in 316L stainless steel that is exposed to primary side coolant, and that this thin membrane is supporting the full system pressure. Discuss the possibility that stress corrosion cracking may occur in this region and give rise to premature activation of this valve. How was this possibility accounted for in the design?

Westinghouse Response:

As identified in the question, the shear section of the automatic depressurization system - stage 4 (ADS-4) squib valve is exposed to primary side coolant, and is subject to full system design pressure. While the shear section has greatly reduced thickness when compared to other pressure retaining portions of the valve, it will be designed in accordance with ASME Code requirements (Sections NB 3500 and NB 3200 analysis). It will also include an appropriate corrosion allowance.

Please note that there is no "severe design notch" in the shear section of this valve. While some pyrotechnic valve designs do incorporate a "V-notch" in the shear section, the shear section in this application actually incorporates a smooth radius con-o-cap intended by design to withstand the design conditions long-term. The con-o-cap reduces the chance of premature cracking.

Westinghouse is still evaluating the best material selection for the application. While 316L stainless steel is the present selection, other materials such as 304L stainless steel are being considered. The final selection will be based on the best experience of Westinghouse and the valve supplier.

Further, Westinghouse notes that there has rarely been an issue of stress corrosion cracking in pressurized water reactor applications when stainless steel materials are used. The condition of hydrogen overpressure and oxygen scavengers provides an environment that is not conducive to stress corrosion cracking.

Design Control Document (DCD) Revision:

None

PRA Revision:

None